Biophysical Journal
Article

Biophysical Society

Full-Spectral Multiplexing of Bioluminescence Resonance Energy Transfer in Three TRPV Channels

Hermanus Johannes Ruigrok,[1,2] Guillaume Shahid,[1,2] Bertrand Goudeau,[2,3] Florence Poulletier de Gannes,[1,2] Emmanuelle Poque-Haro,[1,2] Annabelle Hurtier,[1,2] Isabelle Lagroye,[1,2,4] Pierre Vacher,[2,5] Stéphane Arbault,[2,3] Neso Sojic,[2,3] Bernard Veyret,[1,2] and Yann Percherancier[1,2,*]

[1]Laboratoire de l'Intégration du Matériau au Système, Centre National de la Recherche Scientifique (CNRS) UMR 5218, Talence, France; [2]Université de Bordeaux, Talence, France; [3]Institut des Sciences Moleculaires, Centre National de la Recherche Scientifique (CNRS) UMR 5255, NSYSA Group, ENSCBP, Pessac, France; [4]Paris Sciences et Lettres Research University, Paris, France; and [5]Institut National de la Santé et de la Recherche Médicale (INSERM) U1218, Institut Bergonié, Bordeaux, France

ABSTRACT Multiplexed bioluminescence resonance energy transfer (BRET) assays were developed to monitor the activation of several functional transient receptor potential (TRP) channels in live cells and in real time. We probed both TRPV1 intramolecular rearrangements and its interaction with Calmodulin (CaM) under activation by chemical agonists and temperature. Our BRET study also confirmed that: (1) capsaicin and heat promoted distinct transitions, independently coupled to channel gating, and that (2) TRPV1 and Ca^{2+}-bound CaM but not Ca^{2+}-free CaM were preassociated in resting live cells, while capsaicin activation induced both the formation of more TRPV1/CaM complexes and conformational changes. The BRET assay, based on the interaction with Calmodulin, was successfully extended to TRPV3 and TRPV4 channels. We therefore developed a full-spectral three-color BRET assay for analyzing the specific activation of each of the three TRPV channels in a single sample. Such key improvement in BRET measurement paves the way for the simultaneous monitoring of independent biological pathways in live cells.

INTRODUCTION

Over the last 15 years, resonance energy-transfer approaches have offered new opportunities for real-time probing of the activity of an evergrowing list of proteins in live cells (1). These techniques are based on the nonradiative transfer of energy between an energy donor and a compatible fluorescent energy acceptor. This is a system of choice for monitoring both constitutive and regulated inter- and intramolecular interaction. Among these techniques, bioluminescence resonance energy transfer (BRET) has become a popular, broadly applicable method, particularly useful in molecular pharmacology, especially concerning G protein-coupled receptors (2).

Being able to study multiple molecular events simultaneously with a single measurement represents a significant step forward in biology and medicine. Spectral imaging, coupled to mathematical processing, is becoming the gold standard for multiplexed imaging of intracellular molecular events using fluorescent techniques (3,4). Also, systems coupling multispectral fluorescence imaging with microscopy and flow cytometry are now commercially available. However, until now, the BRET technique was limited to a filter-based approach that hindered its further development. Using transient receptor potential (TRP) ion channels as a model, we report here a full-spectral analysis of multiple-color BRET probes.

TRP proteins form a superfamily of ubiquitously expressed, functionally diverse, cation-permeable channels with varying selectivity to several cations. All TRPs are integral proteins containing six transmembrane domains. The N- and C-terminal domains are intracellular and known to be involved in TRP function, regulation, and channel assembly. TRP channels can be activated by several physicochemical means, including the transduction of chemical, temperature, and mechanical stimuli (5). TRP channels function, therefore, as polymodal signal integrators that respond by changing their open probability. They are highly involved in a variety of human physiological processes, including sensory physiology; cardiovascular, gastrointestinal, and urological functions; as well as immunity and development.

Submitted June 16, 2016, and accepted for publication November 21, 2016.

*Correspondence: yann.percherancier@ims-bordeaux.fr

Editor: Henry Colecraft.

http://dx.doi.org/10.1016/j.bpj.2016.11.3197

As a result, TRP channel dysfunction has been implicated in many diseases, leading to their emergence as highly promising drug targets (6). Among the TRP channels, six are recognized as thermo-TRPs, expressed in primary somatosensory neurons and activated at specific temperatures. TRPV1–4 transduce elevated temperatures, ranging from moderate (TRPV3 and TRPV4) to noxious heat (TRPV1 and TRPV2), while TRPM8 and TRPA1 are activated by moderate and extreme cold, respectively (7).

In this study, we developed intra- and intermolecular BRET-based biosensors for monitoring the real-time heat and chemical activation of TRPV1 channels in live cells. Using these, to our knowledge, new tools, we confirmed that (1) capsaicin (CAPS) and heat promoted distinct transitions, independently coupled to channel gating, and (2) TRPV1 and Ca^{2+}-bound Calmodulin (CaM) but not Ca^{2+}-free CaM were preassociated in resting live cells, while CAPS activation induced both the formation of more TRPV1/CaM complexes and conformational changes. We also extended the intermolecular approach to monitor the chemical activation of both TRPV3 and TRPV4. Finally, using spectral decomposition, we demonstrated the simultaneous monitoring of TRPV1, TRPV3, and TRPV4 ion channel activation in a single assay.

MATERIALS AND METHODS

Plasmids

To generate the BRET constructs, super Yellow Fluorescent Protein (YFP) 2 (8) and Renilla Luciferase II (9) were used to improve the brightness of the assay. They are referred as YFP and Luc for short in the rest of the article. The cDNA of Luc and YFP were first cloned together using a three-piece ligation in the *Bam*HI/*Xho*I site of pcDNA3.1(+) (Invitrogen, Carlsbad, CA), yielding two expression vectors pcDNA3.1 YFP-Luc where YFP was cloned in-fusion at the N-terminal of Luc, and pcDNA3.1 Luc-YFP where Luc was cloned in-fusion at the N-terminal of YFP. Both YFP and Luc were amplified by PCR from the pcDNA3-YFP-EPAC-Luc vector (a kind gift of Pr. Michel Bouvier, Institute for Research in Immunology and Cancer, Montreal, Canada)). Luc was cloned either at the N-terminal of YFP as a *Hin*dIII-*Eco*RI fragment (primers used: Luc_*Hin*dIII_ATG_N-term sense and Luc_no Stop_*Eco*RI_N-term antisense) or at the COOH-terminal of YFP as an *Eco*RI-*Xho*I fragment (primer used: Luc_*Eco*RI_ATG_C-term sense and Luc_*Xho*I_Stop_C-term antisense). In parallel, YFP was cloned either at the N-terminal of Luc as a *Hin*dIII-*Eco*RI fragment (primers used: YFP_*Hin*dIII_ATG_N-term sense and YFP_no Stop_*Eco*RI_N-term antisense) or at the COOH-terminal of Luc as an *Eco*RI-XhoI fragment (primer used: YFP_*Eco*RI_ATG_C-term sense and YFP_*Xho*I_Stop_C-term antisense). The sequence joining Luc and YFP sequence encodes VPVNSGGGGS as a linker, and contains an *Age*I restriction site.

The YFP-hTRPV1-Luc expression vector was obtained by subcloning the human TRPV1 cDNA from the pDONR201-hTRPV1 vector (Harvard Medical School PlasmID Repository, clone HsCD00081472) as an *Eco*RI PCR fragment in the *Eco*RI site of the vector pcDNA3.1 YFP-Luc (primer used: hTRPV1_*Eco*RI_Fus_Sense and hTRPV1_*Eco*RI_Fus_antisense). The hTRPV1-Luc expression vector was obtained by subcloning the cDNA of hTRPV1 as a *Hin*dIII-*Eco*RI fragment in place of the YFP in the *Hin*dIII-*Eco*RI site of the pcDNA3.1 YFP-Luc vector (primer used: hTRPV1_*Hin*dIII_ATG_Sense and hTRPV1_*Eco*RI_Fus_antisense). The Luc-hTRPV3 expression vector was obtained by subcloning the cDNA of hTRPV3 (Harvard Medical School PlasmID Repository, clone HsCD00341603) as an *Age*I-*Xho*I fragment in place of the YFP in the *Age*I-*Xho*I sites of the pcDNA3.1 Luc-YFP vector (primer used: hTRPV3_*Age*I_ATG_Sense and hTRPV3_Stop _*Xho*I _antisense). The hTRPV4-Luc expression vector was obtained by subcloning the cDNA of hTRPV4 (a kind gift of Dr. Aubin Penna, INSERM UMR1085, Group C2M2, Rennes University, France) as a *Bam*HI-*Age*I fragment in place of the YFP in the *Bam*HI-*Age*I site of the pcDNA3.1 YFP-Luc vector (primer used: hTRPV4_*Bam*HI_ATG_Sense and hTRPV4_*Age*I_Fus_antisense). In each case, the sequence joining the cDNA of interest and either Luc or YFP sequence encodes VPVNSGGGGS as a linker.

The cDNA of aquamarine (10) was a kind gift of Dr. Fabienne Mérola (Laboratoire de Chimie Physique, CNRS UMR8000, Université Paris-Sud, Orsay, France). The cDNA of mAmetrine (Plasmid No. 54660) and LssmOrange (Plasmid No. 37130) were obtained from AddGene plasmid repository. The cDNA of aquamarine, mAmetrine and LssmOrange were all subcloned as a *Hin*dIII-*Eco*RI fragment in place of the YFP in the *Hin*dIII-*Eco*RI site of the pcDNA3.1 YFP-Luc vector (primer used: YFP_*Hin*dIII_ATG_N-term sense and YFP_no Stop_*Eco*RI_N-term antisense) to yield pcDNA3.1 FP-Luc expression vectors (FP being any fluorescent protein between aquamarine, mAmetrine, and LssmOrange). The human Calmodulin (CaM) cDNA was a kind gift of Dr. Peter J. McCormick (School of Pharmacy, University of East Anglia, Norwich, UK). A Ca^{2+}-insensitive mutant form of CaM (CaM1234), in which point mutations within all four EF hands eliminate Ca^{2+} binding was a kind gift of Pr. Sharona E. Gordon (University of Washington, Seattle, WA). The YFP-CaM expression vectors were obtained by subcloning the CaM cDNA in place of the Luc at the C-terminus of YFP into the YFP-Luc as an *Eco*RI-XhoI fragment (primers used: hCaM_*Ecor*RI- ATG-Sense and hCaM_Stop_*Xho*_antisense). A similar strategy was used to obtain the FP-CaM expression vector using the pcDNA3.1 FP-Luc expression vector instead of the pcDNA3.1 YFP-Luc.

The sequence of each cDNA construct was confirmed by DNA sequencing.

Primers

YFP and Luc primers

Luc_*Hin*dIII_ATG_N-term sense, TGTCTAAGCTTGGATCCGCCAC CATGACCAGCAAGGTGTACGACCCCGAGC
Luc_no Stop_*Eco*RI_N-term antisense, CACCAGAATTCACCGG TACCTGCTCGTTCTTCAGCACTCTCTCC
Luc_*Eco*RI_ATG_C-term sense, GTGTACCGGTGAATTCTGGTGGA GGCGGATCTATGACCAGCAAGGTGTACGACCCCGAGC
Luc_*Xho*I_Stop_C-term antisense, ATCTAGTCTAGACTCGAGCGGT TACTGCTCGTTCTTCAGCACTCTCTCC
YFP_*Hin*dIII_ATG_N-term sense, TGTCTAAGCTTGGATCCGCCA CCATGGTGAGCAAGGGCGAGGAGCTGTTCACC
YFP_no Stop_*Eco*RI_N-term antisense, CACCAGAATTCACCGGTA CCTTGTACAGCTCGTCCATGCCG
YFP_*Eco*RI_ATG_C-term sense, TGTGTACCGGTGAATTCTGGTG GAGGCGGATCTATGGTGAGCAAGGGCGAGGAGCTGTTC
YFP_*Xho*I_Stop_C-term antisense, ATCTAGTCTAGACTCGAGCGG TTACTTGTACAGCTCGTCCATGCCG

hTRPV1 primers

hTRPV1_*Eco*RI_Fus_Sense, TGTGTACCGGTGAATTCTGGTGGAG GCGGATCTATGAAGAAATGGAGCAGCACAGACT
hTRPV1_*Eco*RI_Fus_antisense, CACCAGAATTCACCGGTACCTTC TCCCCGGAAGCGGCAGGACTC
hTRPV1_*Hin*dIII_ATG_Sense, TGTCTAAGCTTGGTACCGCaCACC ATGAAGAAATGGAGCAGCACAGACT

hTRPV3 primers

hTRPV3_*Age*I_ATG_Sense, TGTCTAAGCTTGGTACCGCCACCATGAAAGCCCACCCCAAGGAGATGG
hTRPV3_Stop _*Xho*I _antisense, ATCTAGTCTAGACTCGAGCGGCTACACCGAGGTTTCCGGGAATTCCTCG

hTRPV4 primers

hTRPV4_*Bam*HI_ATG_Sense, TGTCTGGATCCAAGCTTGCCACCATGGCGGATTCCAGCGAAGGCCCCCG
hTRPV4_*Age*I_Fus_antisense, CACCAGAATTCACCGGTACGAGCGGGGCGTCATCAGTCCTCCACTTGCG

Calmodulin primers

hCaM_*Eco*RI_ATG_Sense, TGTGTACCGGTGAATTCTGGTGGAGGCGGATCTATGGCTGACCAGCTGACTGAGGAGC
hCaM_Stop_*Xho*_antisense, ATCTAGTCTAGACTCGAGCGGTTACTTTGCAGTCATCATCTGTACAAAC

Reagents

CAPS and Capsazepine (CPZ) were all from Tocris (Bristol, UK). Drofenine and GSK1016790A and BAPTA-AM were from Sigma (Lyon, France). AMG517 was from Medchemexpress (Princeton, NJ). Coelenterazine H and Purple Coelenterazine (Nanolight Technology, Pinetop, AZ) were added to a final concentration of 5 μM.

Cell culture and transfections

HEK293T cells were maintained in Dulbecco's modified Eagle's medium—high glucose (Cat. No. D6429; Sigma-Aldrich, St. Louis, MO) supplemented with 10% fetal bovine serum, 100 units mL-1 penicillin and streptomycin. Twenty-four hours before transfection, cells were seeded at a density of 500,000 cells in 6-well dishes. Transient transfections were performed using polyethylenimine (PEI, linear, Mr 25,000; Cat. No. 23966 Polysciences, Warrington, PA) with a PEI/DNA ratio of 4:1, as explained in Percherancier et al. (11). Usually, 0.1–0.25 μg of the donor constructions and 1.75–1.9 μg of the acceptor constructions were transfected for the BRET measurement, except for BRET titration curves, where increasing amounts of YFP-CaM (0.01–2 μg) were transfected with a fixed amount of TRPV1-Luc (0.1 μg). The amount of transfected DNA was completed to a total of 2 μg with pcDNA3.1 empty vector. After overnight incubation, transfected cells were then detached, resuspended in DMEM w/o red phenol (Ref. No. 21063-029; ThermoFisher Scientific, Waltham, MA) and replated at a density of 10^5 cells per well in 96-well white plates with clear bottoms (Greiner Bio One, Courtaboeuf, France) pretreated with D-polylysine (Sigma-Aldrich) for reading with the Tristar2 luminometer (Berthold Technologies, Bad Wildbad, Germany) or onto 12 mm diameter glass coverslips (Knittel Glass, Braunschweig, Germany) treated with poly-L-lysine for the reading with the SpectraPro 2300i spectrometer (Acton Optics, Acton, MA) (see below). Cells were left in culture for 24 h before being processed for the BRET assay.

Filter-based BRET assays

For the pharmacological characterization of the probes, agonists and Coelenterazine H were directly added to the cells and BRET assays were performed using a multidetector TriStar2 LB942 microplate reader (Berthold Technologies) for sequential integration of the signals emitted by the total cell population in each well measured, and detected at 480 ± 20 nm and 540 ± 40 nm for the Luc (energy donor) and YFP (energy acceptor) light emissions, respectively. The BRET signal was determined by calculating the ratio of the emission intensity measured in the acceptor window (I_{acceptor}) over the emission intensity measured in the donor window (I_{donor}), according to Eq.1:

$$BRET = \frac{I_{\text{acceptor}}}{I_{\text{donor}}}. \quad (1)$$

Due to the overlapping emission spectra of Luc and YFP, a fraction of the light detected in the YFP filter originates from the Luc emission, resulting in a contaminating signal (12). The Net BRET is defined as the BRET ratio of cells coexpressing Luc and YFP constructs minus the BRET ratio of cells expressing only the Luc construct in the same experiment.

To assess the functionality of the probes based on the TRPV channels, agonists and antagonists were added as described in the text for 3 min at given temperature before the addition of Coelenterazine H and BRET reading. All experiments were performed at 37°C and pH 7.5 unless otherwise indicated.

Spectral BRET assays

Full BRET spectra were acquired using an optical fiber linked to a Spectra Pro 2300i spectrometer (Princeton Instruments, Acton, MA), equipped with a liquid-nitrogen-cooled charge-coupled device camera for recording the full visible spectrum (Acton Optics). The bioluminescent signal was recorded from transfected cells seeded onto a glass coverslip and placed into a white opaque measurement chamber made of Teflon and containing an isotonic solution (NaCl 145 mM, KCl 5 mM, KH_2PO_4 4 mM, $CaCl_2$ 1 mM, $MgSO_4$ 1 mM, Glucose 10 mM) adjusted to pH7.5. The temperature of the cell buffer was regulated using an Eppendorf ThermoStat Plus and measured in real time using a fiber-optic temperature measurement Luxtron 812 system (Lumasense Technologies, Santa Clara, CA). All experiments were performed at 37°C unless otherwise indicated.

Using the LabView programming language (National Instruments, Austin, TX), an interface was developed to acquire the bioluminescent spectra and perform real-time spectral decomposition of the BRET signal into its various components. The experimental emission spectra of Luc (with either coelenterazine H or purple coelenterazine as the substrate), YFP, mAmetrine, aquamarine, and Lss-mOrange were first obtained experimentally using a Cary Eclipse Fluorimeter (Agilent Technologies, Santa Clara, CA) (Figs. S1 and S2 in the Supporting Material). Each spectrum was then fitted as a linear combination of Gaussian curves based on

$$y(\lambda) = \sum_{i=1}^{n} a_i e^{-\frac{(\lambda - \lambda\, max_i)^2}{2\sigma_i^2}}, \quad (2)$$

where λ is the wavelength, a_i values are the peak heights of the Gaussian curves, $\lambda\, max_i$ values are the wavelengths of their peaks, and σ_i are the widths at half-maximum.

For each time point, the full BRET spectrum was calculated using Eq. 3 for experiments using Luc (and coelenterazine H) as energy donor and YFP as energy acceptor, or using Eq. 4 for Luc (and purple coelenterazine) as energy donor, and aquamarine, mAmetrine, and Lss-mOrange as energy acceptors,

$$Y = k_{\text{Luc}} y_{\text{Luc}} + k_{\text{YFP}} y_{\text{YFP}}, \quad (3)$$

$$Y = k_{\text{Luc}} y_{\text{Luc}} + k_{\text{aquamarine}} y_{\text{aquamarine}} + k_{\text{mAmetrine}} y_{\text{mAmetrine}} + k_{\text{Lss mOrange}} y_{\text{Lss mOrange}}, \quad (4)$$

and where k_{probe} values are the probe coefficients.

The difference between the experimental spectrum and the linear combination Y of donor and acceptor spectra was minimized, with respect to the k_{probe} coefficients, using a standard iterative algorithm based on a nonlinear

least-square fitting method developed by Levenberg (13). Using this algorithm for each time point, it was straightforward to calculate the actual BRET ratio for each probe by dividing the area under the acceptor spectrum by that of the donor spectrum. This analysis method represents a major advantage over the standard, filter-based method, for calculating the BRET ratio (12), avoiding the contamination of the acceptor signal by the donor emission. The results of the decomposition of the BRET spectra obtained when measuring the bioluminescent signal from a cell population expressing either the YFP-Luc, the aquamarine-Luc, the mAmetrine-Luc, or the Lss-mOrange fusion proteins are given in Fig. S3. All experiments were performed at 37°C unless otherwise indicated.

For experiments under temperature rise, in which the spectral decomposition approach was used along with the SpectraPro 2300i (Princeton Instruments) the area of YFP and Luc emission spectra were corrected for the subtle changes observed between 25 and 50°C (Fig. S2). We calculated that YFP emission diminished linearly by 0.46% per °C within the temperature range comprised between 25 and 50°C, while the shape of the spectra was not modified. The YFP emission spectra area was therefore corrected for the temperature-induced variation from 25 to 50°C, according to

$$A_{T\mathrm{corr}} = A_T + A_T(T-25) \times \frac{0.46}{100}, \quad (5)$$

where T is any temperature between 25 and 50°C, A_T is the area of the YFP spectra measured at temperature T, and $A_{T\mathrm{corr}}$ is the corrected area of YFP at the temperature T.

We calculated that Luc emission spectra shape was slightly modified on its red part inducing a linear increase of 0.17% per degree of its area within the temperature range comprised between 25 and 50°C (Fig. S2). The Luc emission spectra area was therefore corrected for the temperature-induced variation from 25 to 50°C, according to

$$B_{T\mathrm{corr}} = B_T - B_T(T-25) \times \frac{0.17}{100}, \quad (6)$$

where T is the temperature between 25 and 50°C, B_T is the area of the Luc spectrum measured at temperature T, and $B_{T\mathrm{corr}}$ is the corrected area of Luc at temperature T.

Under temperature rise, the evolution of luminescence counts clearly indicates that the luciferase enzyme activity is improved when the temperature is raised from 25 to 40°C, and then decrease up to 50°C, but remained above the limit of sensitivity of the spectrometer. (Fig. S4).

Calcium assays

HEK cells were loaded with 0.67 μM FuraPE3-AM (Teflabs, Austin, TX) for 30 min at 37°C in Hank's Balanced Salt Solution. After washing with PBS, fresh Hank's Balanced Salt Solution was added to the cells and calcium measurement was performed at 37°C using a Flexstation II (Molecular Devices, Sunnyvale, CA). Fura2-AM was alternately excited at 340 and 380 nm and emission was read at 510 nm. The 340:380 nm ratio was used to estimate the variations of cytosolic calcium concentration.

Data analysis

Data obtained in BRET and calcium assays were analyzed using the software Prism 6.01 (GraphPad Software, La Jolla, CA). Sigmoidal dose-response curves were fitted using:

$$Y = Bottom + \frac{(Top - Bottom)}{1 + 10^{LogEC50-X}}, \quad (7)$$

where X is the logarithm of agonist concentration and Y is the response; *Bottom* is the Y value at the bottom plateau; *Top* is the Y value at the top plateau; and LogEC50 is the X value when the response is halfway between *Bottom* and *Top*.

RESULTS

Validation of the TRPV1 BRET biosensors

Knowing that: 1) fluorescence resonance energy transfer (FRET) analysis revealed that movements within intracellular regions of the TRP-structurally related Kv2.1 channel were part of the gating machinery (14) and 2) TRPV1 contains CaM binding sequences (15,16), we hypothesized that BRET could be used to monitor TRP channel activation in live cells. TRPV1, the most studied channel in the TRP family, was therefore used as our main model for probing channel conformational changes and CaM docking after activation. For this purpose, we developed two proximity-based BRET assays, relying on the energy donor *Renilla reniformis* luciferase (Luc), fused to the C-terminus part of the TRPV1 protein, and the energy acceptor Yellow Fluorescent Protein (YFP), fused to the N-terminus part of either TRPV1-Luc or CaM. In the first case, the TRPV1 protein was sandwiched between the YFP and Luc groups, resulting in an intramolecular BRET probe, referred to below as YFP-TRPV1-Luc (Fig. 1 *A*), while, in the second case, YFP-CaM docking on TRPV1-Luc (TRPV1-Luc/YFP-CaM) was monitored (Fig. 2 *A*).

TRP channel activation was evaluated in transfected HEK293T human embryonic-kidney cells. We first assessed whether, after transfection, our TRPV1-fusion proteins remained functional despite the N- and/or C-terminus addition of the YFP or Luc groups. For this purpose, we measured calcium entry in mock-transfected or transfected HEK293T cells with either native TRPV1 or the BRET constructs, YFP-TRPV1-Luc or TRPV1-Luc. After exposure to CAPS, the prototypical TRPV1 agonist, a rapid, maintained increase in cytosolic calcium concentration was observed in cells expressing TRPV1, YFP-TRPV1-Luc, or TRPV1-Luc, but not in mock-transfected cells (Fig. S5). This indicated that the addition of either the YFP and/or Luc groups did not hinder TRPV1 channel opening, in agreement with previous data (17,18). HEK293T cells expressing YFP-TRPV1-Luc (Fig. 1) or TRPV1-Luc/YFP-CaM (Fig. 2) were then processed for BRET analysis. In both cases, the basal BRET, measured in resting condition, increased with first-order kinetics after exposure to CAPS (Figs. 1 *B* and 2 *B*).

The increase in basal BRET, measured using the intramolecular TRPV1 BRET probe, probably reflected the changes in the various modes of energy transfer between Luc and YFP inside the TRPV1 tetrameric organization of the channel during channel opening (18–20). However, the increase in basal BRET between TRPV1 and Calmodulin was more elusive, resulting either from a conformational change in a preassembled TRPV1-CaM complex and/or a modification

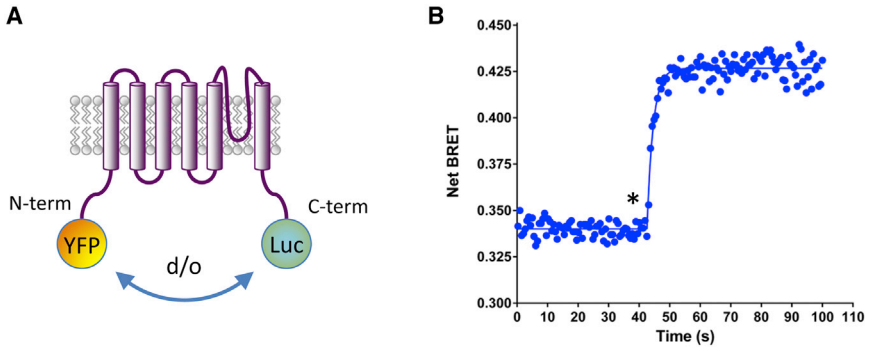

FIGURE 1 Measuring TRPV1 activity using an intramolecular BRET probe (*A*). Schematic representation of the YFP-TRPV1-Luc intramolecular BRET probe, where YFP was fused to the N-terminal extremity of TRPV1 while Luc was fused to the C-terminal extremity of TRPV1. After activation of TRPV1, the distance (*d*) and/or the orientation (*o*) between Luc and YFP were expected to be modified. (*B*) Kinetic measurement of the effect of 20 μM CAPS on HEK293T cells expressing the YFP-TRPV1-Luc BRET probe. (*Star*) Time of CAPS injection. Data represent one out of five independent experiments. The time-constant (τ) of the BRET increase induced by CAPS is 2.01 $\pm$ 0.29 s, $n = 5$. To see this figure in color, go online.

in the association-dissociation equilibrium between these two partners. Interestingly, both chelation of the intracytoplasmic calcium pool using BAPTA-AM or the use of a YFP-tagged Ca^{2+}-insensitive mutant form of CaM (YFP-CaM1234; Rosenbaum et al. (15)) as an acceptor, severely diminished the basal BRET and abolished the CAPS-induced BRET increase. These results indicated that TRPV1 and a pool of calcium-bound CaM were preassociated in resting state and that calcium-bound CaM was essential to observe the CAPS-induced BRET increase in our TRPV1-Luc/YFP-CaM intermolecular BRET assay. To further characterize the interaction between TRPV1 and CaM, we performed BRET titration curves of the TRPV1-Luc/YFP-CaM BRET pair in the presence and absence of CAPS. As shown in Fig. 2 *C*, in the absence of CAPS, the BRET ratio increased as a hyperbolic function of the YFP-CaM/TRPV1-Luc ratio, thus indicating a specific protein-protein interaction (11,12,21). The selectivity of the measured signal was further supported by the fact that coexpression of TRPV1-Luc with either YFP-CaM1234 or YFP alone led to a weaker signal that progressed linearly over the same energy acceptor/donor range. Because random molecular collisions that may give rise to bystander BRET have been shown to increase nearly linearly over a wide range of YFP/Luc (11,12,21), this last result definitely indicated that TRPV1 did not interact with calcium-free CaM. The addition of CAPS dramatically increased the maximal BRET ($BRET_{max}$) observed and slightly, but significantly, affected the shape of the curve, thus reducing the concentration of YFP-CaM needed to reach 50% of the maximal BRET ratio ($BRET_{50} = 493 \pm 146$ under control conditions but 218 ± 58 with CAPS activation, $p < 0.05$). As $BRET_{50}$ represents the propensity of the BRET partners to interact with one another (i.e., their relative affinity) (11,12,21), our data indicated that the CAPS treatments increased the number of TRPV1/CaM complexes. The increase in the $BRET_{max}$ also indicated that CAPS activation induced conformational changes within preformed TRPV1/CaM complexes that affected the distance between the energy donor and acceptor and/or their orientation. Again, no BRET changes were observed upon CAPS activation using either TRPV1-Luc/YFP-CaM1234 or TRPV1-Luc/YFP BRET pairs. Finally, ionomycin had no effect on the TRPV1/CaM basal BRET, suggesting that TRPV1 needs

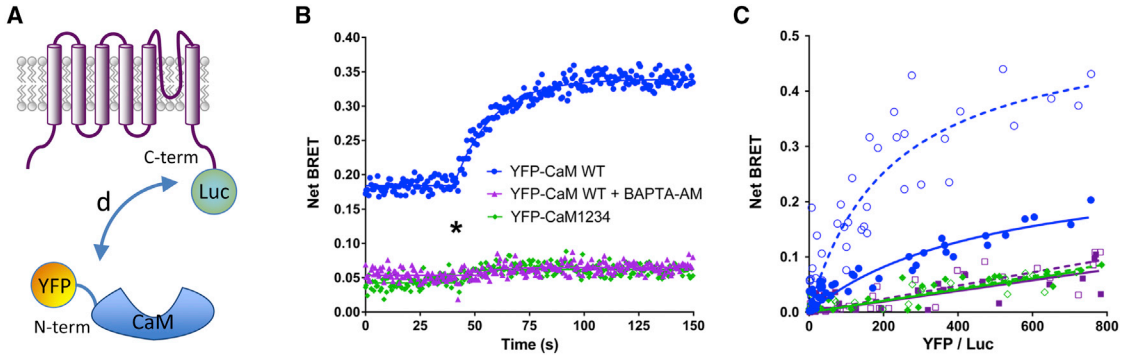

FIGURE 2 Measuring TRPV1 activity using an intermolecular BRET probe. (*A*) Schematic representation of the intermolecular BRET between TRPV1 and Calmodulin. YFP was fused to the N-terminal of Calmodulin and Luc to the C-terminal of TRPV1. After activation of TRPV1, the distance *d* between Luc and YFP was expected to be modified. (*B*) Kinetic measurement of the effect of 20 μM CAPS on cells expressing TRPV1-Luc and either YFP-CaM WT or YFP-CaM1234, pretreated or not with 10 μM BAPTA-AM for 30 min before activation with CAPS. (*Star*) Time of CAPS injection. Data represent one out of three independent experiments. (*C*) Titration assays using HEK293T cells transfected with increasing amounts of YFP-CaM WT (*circles*), YFP-CaM1234 (*diamonds*), or unfused YFP (*square*) and a fixed amount of TRPV1-Luc. Transfected cells were activated (*open symbols*) or not (*solid symbols*) with 20 μM CAPS before BRET reading. Results represent the data obtained over three independent experiments performed in duplicate. To see this figure in color, go online.

to be activated first to engage more Calcium-bound CaM at a later time (Fig. S6).

We next confirmed that the agonist-induced increase in BRET was dose dependent with half-maximal responses (Fig. 3; Table S1) consistent with those reported in the literature, using patch-clamp or calcium-flux measurements on cells expressing endogenous or overexpressed TRPV1 (22,23). The pharmacological selectivity of the ligand-promoted BRET changes was further demonstrated by the competitive nature of the effects, as both CPZ and AMG517, two well-known TRPV1 competitive antagonists, inhibited the CAPS-induced BRET increase, as illustrated by the shift in CAPS potency to higher values in both intra- and intermolecular BRET tests (Fig. 3; Table S1). Altogether, these data strongly suggested that the agonist-promoted BRET changes in both probe configurations corresponded to an activation of TRPV1 channels in live cells.

Heat activation of TRPV1 monitored by BRET

Another series of experiments assessed the effect of temperature on our BRET probes. BRET was measured in real time while heating the cell culture from 25 to 50°C (Fig. 4, *A* and *B*). In cells expressing the TRPV1-Luc/YFP-CaM construct, the basal BRET remained stable between 25 and 37°C. It then increased between 37 and 45°C before reaching a plateau. When the same assay was repeated in a calcium-free buffer or when the cells were preincubated with CPZ, there was no significant change in BRET (Fig. 4 *A*), indicating that the increase observed was fully related to temperature-dependent channel activation and calcium entry through the channel. In cells expressing YFP-TRPV1-Luc, the BRET remained stable up to 37°C, then decreased dramatically up to 50°C (Fig. 4 *B*). Preincubation with CPZ before heating completely modified the temperature-dependent behavior of the YFP-TRPV1-Luc probe: the basal BRET was stable up to 37°C but increased dramatically from 37 to 47°C, before decreasing sharply up to 50°C. Considering that CPZ blocks the opening of the channel over this temperature range (Fig. 4 *A* and McIntyre et al. (24)), these results indicated that TRPV1 underwent some complex temperature-dependent conformational changes despite the channel remaining in the closed state. In a control experiment, raising the temperature from 25 to 50°C yielded either a weak increase in BRET value in HEK293T cells expressing the YFP-Luc fusion protein (9% increase between 25 and 50°C), or almost no effects in HEK293T cells expressing the CD95-Luc/CD95-YFP BRET probes for the Fas-ligand receptors (Fig. S7). No dramatic drop of the signal was measured, in comparison with the YFP-TRPV1-Luc intramolecular BRET probe. Along with the fact that bioluminescence of Renilla luciferase activity is still measurable when cells are heated (Fig. S4), these results indicate that temperature up to 50°C does not significantly alter the energy transfer between Luc and YFP and further confirm the specificity of the heat response measured with both YFP-TRPV1-Luc and TRPV1-Luc/YFP-CaM BRET probes.

Because it has been proposed that the various TRPV1 activation modes are independently coupled to channel gating (25), we investigated whether heating sensitized TRPV1 to CAPS. Using both probes, a temperature rise from 25 to 42°C resulted in both a leftward shift in CAPS potency and an increase in maximal efficacy (Figs. 4, *C* and *D*; Fig. S8). This observation was in agreement with previous studies using the patch-clamp technique (26) and indicated that the temperature response of both YFP-TRPV1-Luc and TRPV1-Luc/YFP-CaM mimicked that of the native TRPV1 channel. Both intra- and intermolecular probes were thus equally well suited to monitoring TRPV1 channel activity. Because TRP channels are known to engage a large network of protein-protein interactions under resting or activated conditions (27), the

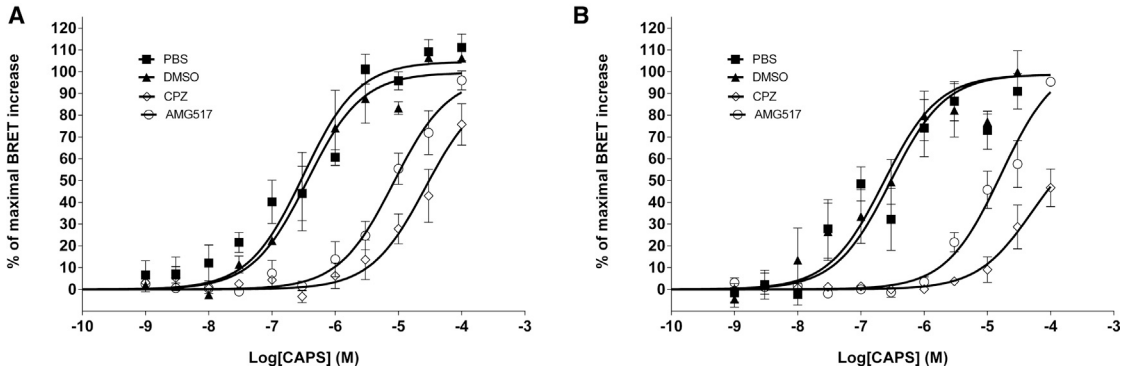

FIGURE 3 Dose-response curves of CAPS-induced BRET changes measured in HEK293T cells expressing the YFP-TRPV1-Luc BRET probe (*A*) or the TRPV1-Luc/YFP-CaM constructs (*B*). Before CAPS activation, the cells were preincubated with either PBS, DMSO (vehicle), 1 μM CPZ, or 1 μM AMG517. In the presence of CPZ or AMG517, but not in the presence of the vehicle alone, the dose-response curve shifted to higher values and the EC_{50} was displaced by more than one order of magnitude (see also Table S1). Results represent the mean ± SE of four independent experiments done in duplicate.

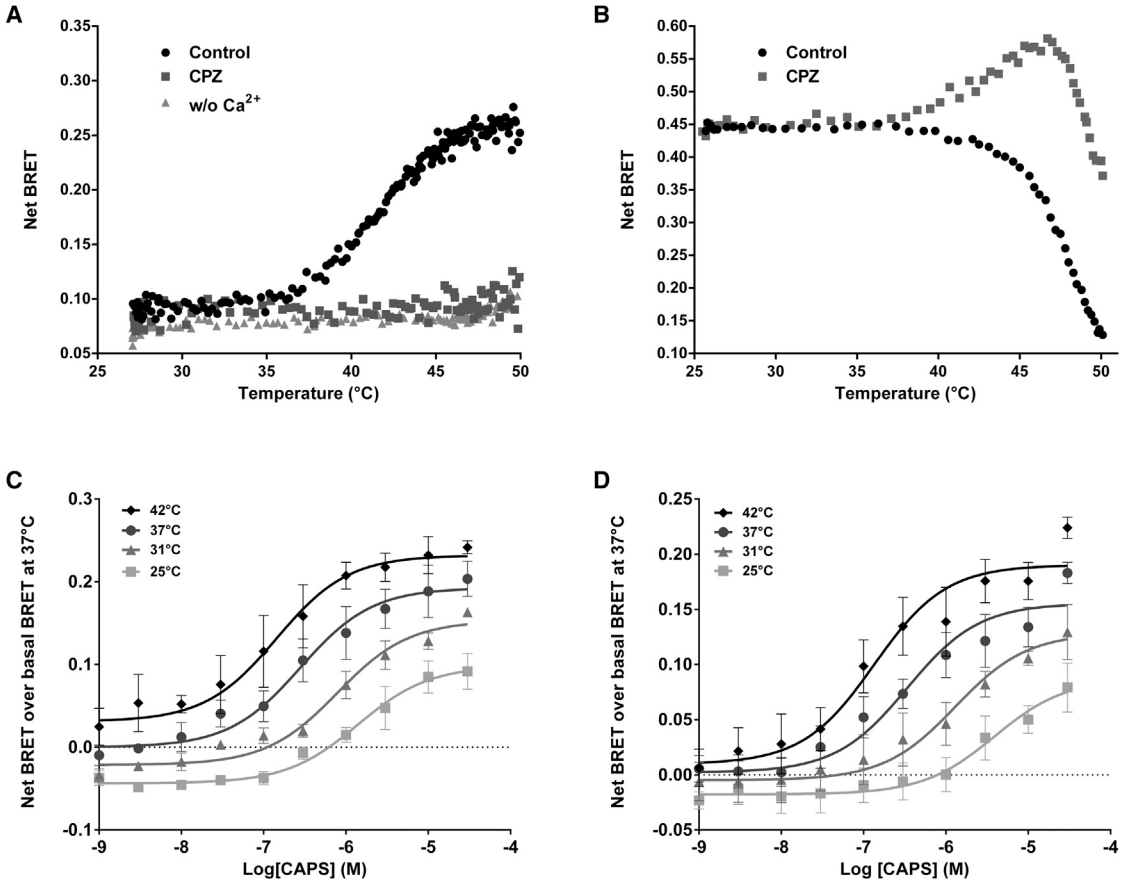

FIGURE 4 Effect of temperature on the pharmacological properties of TRPV1 and its activation, measured by BRET. (*A* and *B*) BRET ratios of HEK293T cells expressing either the TRPV1-Luc/YFP-CaM constructs (*A*) or the YFP-TRPV1-Luc BRET probe (*B*) were recorded in real time while the cell-culture medium was heated from 25 to 50°C using a Peltier plate. The effects of calcium-free extracellular medium (*A*) or preincubation of cells with 1 μM CPZ (*A* and *B*), were also tested. BRET ratios were corrected for the minor variation in Luc and YFP emissions due to the temperature increase (see Materials and Methods). In (*A*), the fact that the signal remained stable over the whole temperature range under Calcium-depleted conditions and in the presence of CPZ further excluded any bias in BRET measurements due to the denaturation of the Luc or YFP groups. Data represent one out of three independent experiments. (*C* and *D*) CAPS dose response curves measured by BRET using HEK293T cells, expressing either the TRPV1-Luc/YFP-CaM constructs (*C*) or the YFP-TRPV1-Luc BRET probe (*D*), incubated at 25, 31, 37, or 42°C. Results represent the mean ± SE of four independent experiments done in duplicate and are expressed as the difference between the net BRET measured in each condition and the basal BRET measured without any agonist at 37°C.

intermolecular-based approach is more promising for studies on CaM-interacting channels or other signaling pathways, while the intramolecular probe is more appropriate for structure-function studies.

Extending the CaM interaction BRET test to TRPV3 and TRPV4 monitoring

The final aim of this work was to monitor the concomitant activation of up to three TRP channels. Consequently, knowing that TRPV3 and TRPV4 also interact with CaM (28), we monitored the activation of TRPV3 and TRPV4 by their specific agonists using the CaM BRET probe approach. As shown in Fig. 5, a dose-dependent increase in BRET between YFP-CaM and Luc-TRPV3 was observed when the transfected cells were challenged with Drofenine, a specific TRPV3 agonist, yielding an EC_{50} of 206 μM in agreement with Deering-Rice et al. (29). We found no dose-dependent BRET increase when the same cells were challenged with either the TRPV1-specific agonist CAPS or the TRPV4-specific agonist GSK1016790A. Similarly, a dose-dependent increase in the TRPV4-Luc/YFP-CaM basal BRET was observed when the transfected cells were challenged with GSK1016790A, yielding an EC_{50} of 1.93 nM, also in agreement with Jin et al. (30). As shown for TRPV3, cross activation of TRPV4-Luc/YFP-CaM-expressing cells with either CAPS or Drofenine did not produce any increase in the basal BRET. We also showed that TRPV1-Luc/YFP-CaM interaction was sensitive to CAPS, but not to Drofenine or GSK1016790A (Fig. 5). These results demonstrated the effectiveness and flexibility of the CaM-binding BRET test for monitoring the chemical activation of CaM-interacting TRP channels.

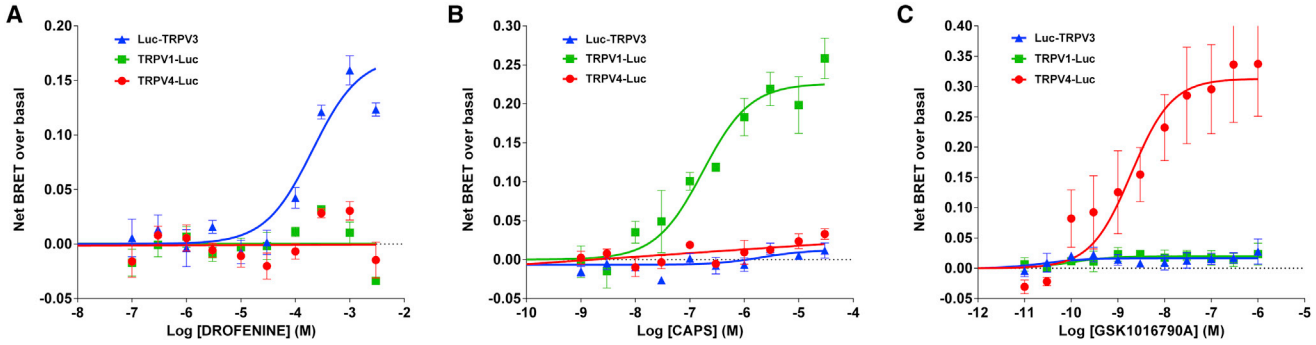

FIGURE 5 Dose-response curve of the effect of Drofenine (*A*), CAPS (*B*), and GSK1016790A (*C*) on HEK293T cells coexpressing YFP-CaM and Luc-TRPV3 (*triangle*), TRPV1-Luc (*square*), or TRPV4-Luc (*circle*). Results are expressed as the difference between the net BRET measured in each condition and the basal BRET measured without any agonist. Basal BRETs of 0.221 ± 0.004, 0.202 ± 0.003, and 0.275 ± 0.008 were measured in resting HEK293T cells expressing Luc-TRPV3/YFP-CaM, TRPV1-Luc/YFP-CaM, and TRPV4-Luc/YFP-CaM, respectively. As mentioned for TRPV1, these results potentially indicate that TRPV3 and TRPV4 interacted with CaM under nonactivated conditions. Results represent the mean ± SE of three independent experiments done in duplicate. To see this figure in color, go online.

Multiplexed BRET monitoring of three TRPV channels using spectral decomposition

We then designed a single test to monitor the activity of several TRP channels simultaneously. The standard filter-based BRET approach constituted a technological barrier to performing a multicolor BRET assay with more than two colors. We therefore extended the BRET full-spectral analysis, already implemented for one acceptor (Fig. 4, *A* and *B*; see Materials and Methods), to analyze three acceptors. For this purpose, a blue-shifted coelenterazine was used to improve acceptor separation, as demonstrated in the BRET2 configuration (31). However, because the advantages associated with the BRET2 system were partly offset by the low quantum yield and rapid decay kinetics of the coelenterazine-400a donor substrate, we used the recently developed methoxy e-Coelenterazine, also known as "purple coelenterazine", that yields up to 13 times more luminescence, with a maximal emission at 425 nm (32). Moreover, Renilla Luciferase II was used as a donor, as this mutant yields luminescence signals 50 times brighter than those generated by the wild-type (9).

It is known that aquamarine, mAmetrine, and LSSmOrange are all fluorescent proteins, excitable in the 400–430 nm range, with sufficiently different Stoke's shifts to provide good separation of their emission spectra (10,33–35; Fig. S1). We verified experimentally that the bioluminescence emission spectrum of the Luc enzyme in the presence of purple coelenterazine substrate matched the excitation spectra of aquamarine, mAmetrine, and LSSmOrange (Fig. S1). As previously done for YFP, we modeled the shape of the spectra of aquamarine, mAmetrine, and LSSmOrange and implemented them in our spectral BRET analysis (see Materials and Methods). The HEK293T cell populations expressing aquamarine-Luc, mAmetrine-Luc, or LSSmOrange-Luc fusion proteins were then mixed in one dish and the multicomponent BRET spectrum was acquired. Our algorithm fitted a theoretical function to the experimental data obtained, which intrinsically contained the functions of all components (Fig. 6 *A*). It was then straightforward to calculate the BRET ratio for each probe by dividing the area of the respective acceptor spectrum by that of the donor spectrum. We then mixed together HEK293T cells expressing Luc-TRPV3/aquamarine-CaM, TRPV1-Luc/mAmetrine-CaM and TRPV4-Luc/LSSmOrange-CaM and performed the spectral decomposition of the complex multicolored BRET signal, during agonist activation, in real time. As shown in Fig. 6, *B–D*, this three-color spectral BRET analysis revealed the selective activation of each TRPV channel in a single well. In each case, agonist stimulation induced a specific increase in its cognate TRPV BRET probe signal. Drofenine injection induced an increase in only the TRPV3-related BRET ratio (Fig. 6 *B*), while activation with CAPS or GSK1016790A induced a time-dependent increase in only the TRPV1- or TRPV4-related BRET ratio, respectively (Fig. 6, *C* and *D*).

DISCUSSION

We report here the characterization of probes for real-time BRET measurement of TRPV1, TRPV3, and TRPV4 ion-channel activation in live cells. A decomposition of the whole emission spectrum of the BRET signal, instead of the usual selective filter-based approach, provided a reliable method for performing three-color BRET tests. This, to our knowledge, novel approach was used to observe the selective activation of TRPV1, TRPV3, and TRPV4 in a single assay, simultaneously, in real time.

The FRET technique, based on intra- and intermolecular probes, has previously been used to probe conformational changes in various channels in live cells or membranes during activation (36). Alternatively, FRET has also been applied to studying the interactions of some ion channels

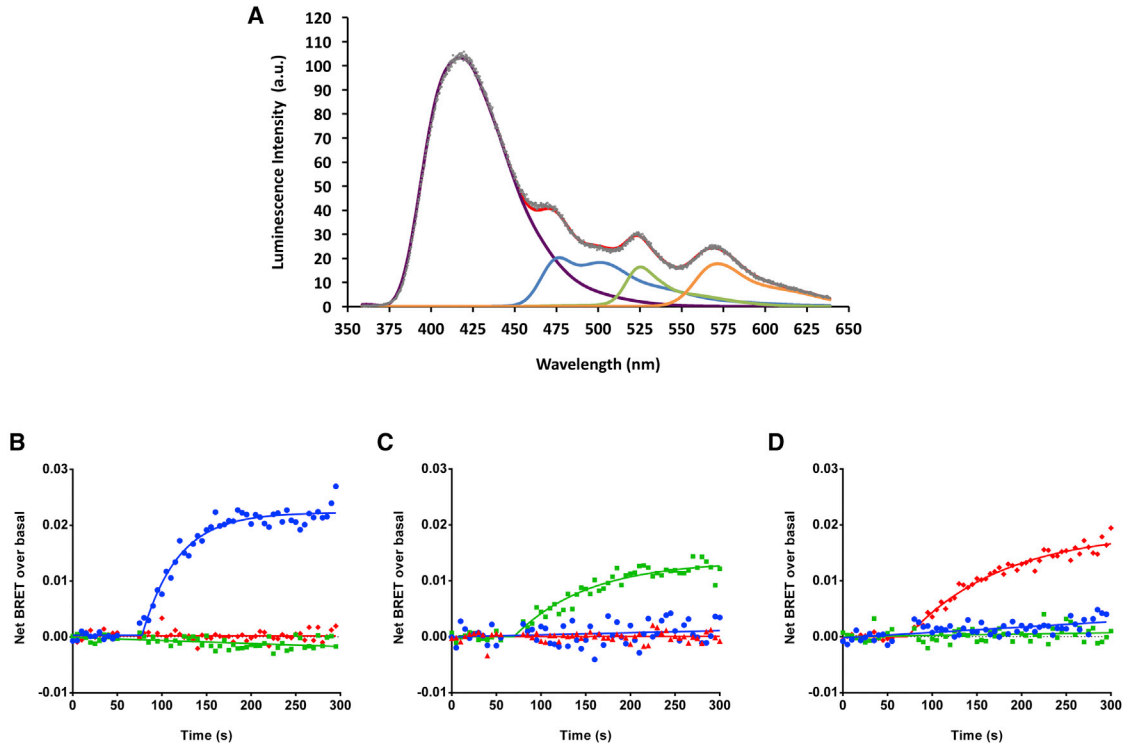

FIGURE 6 Multiplexing measurements of TRPV activity using multicolor BRET. (*A*) Example of a three-color BRET spectrum and its decomposition, measured in a coculture containing three HEK293T subpopulations transfected with aquamarine-Luc, mAmetrine-Luc, or LSSmOrange-Luc. (*Gray dots*) Experimental data. (*Red line*) Best fit to the experimental data. (*Purple*, *blue*, *green*, and *orange lines*) Spectral components of Luc, aquamarine, mAmetrine, and LSSmOrange, respectively. (*B–D*) Multicolored BRET produced by Luc and aquamarine, Luc and mAmetrine, and Luc and LSSmOrange were measured in real time in one sample containing a mixed population of cells expressing Luc-TRPV3/aquamarine-CaM (*blue line*, basal BRET of 0.027 ± 0.002), TRPV1-Luc/mAmetrine-CaM (*green line*, basal BRET of 0.015 ± 0.001), and TRPV4-Luc/LSSmOrange-CaM (*red line*, basal BRET of 0.017 ± 0.001) constructs. One mM Drofenine (*B*), 20 μM CAPS (*C*), or 100 nM GSK101 (*D*) were injected 75 s after the beginning of the experiment initiated by the injection of purple coelenterazine into the buffer. Results represent the mean of three independent experiments.

with partners, such as Calmodulin (37–40). These assays offer the advantage of single-cell microscopy imaging that may be combined with voltage-clamp conditions, thus providing a precise control of channel activation while recording the FRET signal. However, eliminating the need for an external light source for donor excitation gives BRET some advantages over FRET: it does not cause photodamage to cells, photobleaching of fluorophores, background autofluorescence, or direct excitation of the acceptor (41). Thanks to these advantages, the BRET technique has been widely implemented for drug screening, especially in the G protein-coupled receptor research field (2). Implementation of high-throughput screening on ion channels, including TRPs, has proved more problematic (42). The gold standard for evaluating the activity of TRPs and other ion channels is patch-clamp electrophysiology. Improvements are rapidly emerging to increase throughput for the direct screening of ion channel targets, including TRP channels, by using automated electrophysiology and planar patch-clamp techniques (43). These approaches remain expensive and require expert handling. Moreover, whereas BRET experiments offer the advantage of using intact cells, the whole-cell recording configuration of the patch-clamp technique leads to washout of the cytosol by the saline solution in the patch pipette. In addition, mechanical constraints due to pipette positioning on the cell membrane and negative pressure may introduce bias in the measurement of mechanosensitive channel activities, including some TRP channels. For high-throughput screening, indirect readout technologies are often used as an initial screening step, later confirmed by patch-clamp. These techniques usually rely on fluorescent assays to monitor changes in membrane potential or intracytoplasmic calcium concentrations (42,44). Nonetheless, indirect assays of ion channel function often produce false-positive hits, as they monitor endpoints distal from the channel, separated by multiple steps in the signaling pathways. Measuring events proximal to receptor activation reduces the probability of false positives. Therefore, the advent of BRET probes for monitoring the activation of channels in live cells in real time is most valuable.

While steady-state TRPV1 subunit oligomerization had been previously studied using either FRET (18), or a combination of BiMolecular Fluorescence complementation and BRET (20), none of these authors could show any variation of the measured signal after TRPV1 activation. Several

studies succeeded in measuring ion-channel activation using intra- or intermolecular FRET based probes (14,36), but only one research group successfully reported the use of BRET-based biosensors to monitor ion-channel activity, focusing on the Kir3 inwardly rectifying potassium channel in combination with fluorescein arsenical hairpin binder (FlAsH) (45). Adapting the FlAsH/BRET approach to other channels would require extensive studies to determine how to insert the FlAsH sequence into the channel structure to yield optimal variation in the BRET ratio upon channel activation. Moreover, variations in the BRET ratio reported by Robertson et al. (45) were often weak, not exceeding 5–10% of the basal BRET. In sharp contrast, our experiments using TRPV-Luc/YFP-CaM detected significantly larger increases upon activation, ranging from 65 to 115% of the corresponding basal net BRET (Fig. 5). These probes open up, to our knowledge, new prospects for developing simple cell-based assays that provide direct information on channel activity, especially in drug screening.

Our study sheds, to our knowledge, new light on the interaction between CaM and TRPV1. Calmodulin has been identified as a component of the TRPV1 inactivation machinery, although discrepancies remain regarding the Ca^{2+} dependence for TRPV1 interaction, as well as its binding site on TRPV1 (15,16,46,47). Using disruptive biochemical techniques, Lau et al. (47) showed that Ca^{2+}-bound CaM, but not Ca^{2+}-free CaM, interacted with one of the unconventional TRPV1 channel CaM binding sites. In contrast, Rosenbaum et al. (15) reported that the fraction of CaM bound to TRPV1 remained unchanged in the presence or absence of Ca^{2+}. Our TRPV1-Luc/YFP-CaM intermolecular BRET assay demonstrated that TRPV1 and Ca^{2+}-bound CaM were preassociated in resting living cells. Our results also confirmed the observation by Numazaki et al. (16) that more TRPV1-CaM complexes were formed upon CAPS activation. The BRET titration curves clearly indicated that no specific interaction occurred between TRPV1 and Ca^{2+}-free CaM, even after CAPS activation. Finally, our results indicated that conformational changes occurring during CAPS activation of TRPV1 impacted the distance between Luc on TRPV1-Luc and YFP on YFP-CaM proteins and/or their orientation, leading to a higher maximal BRET.

In these experiments, the intramolecular BRET probe was not used to investigate TRPs other than TRPV1, but represented a promising tool for elucidating TRPV1 gating. We observed that, while CAPS treatment induced an increase in the basal BRET of YFP-TRPV1-Luc, heating produced multiple conformational changes (Figs. 1 and 4). In agreement with Yang et al. (48), this indicated that CAPS and heat triggered distinct conformational transitions, both resulting in channel-pore opening.

A voltage-sensitive mechanism was initially proposed to underlie thermosensitive TRP channel gating (49,50). According to this hypothesis, thermal and chemical stimuli act to increase the intrinsic voltage sensitivity of TRP channels. Nonetheless, an allosteric model in which voltage, temperature, agonists, and inverse agonists are independently coupled, either positively or negatively, has proved to be a more accurate description of many aspects of TRPV1 gating (23,25). We also observed that heat increased CAPS potency and efficacy, using both intra- and intermolecular BRET tests. Altogether, our results are in full agreement with the findings that CAPS and heat promote distinct transitions that are allosterically coupled during channel pore gating (23,25).

The fact that a simple BRET assay was capable of monitoring the chemical activation of three TRPV channels in turn prompted us to measure TRPV1, TRPV3, and TRPV4 activities in a single assay. One of the greatest obstacles to achieving quantitative multiplexed BRET measurements is the overlap among donor and acceptor emission spectra. The usual approach to by-pass this technical barrier, using a two-color BRET assay, is to fine-tune filter sets for sequential measurement of the energy transfer between Luc and two fluorescent acceptors with sufficiently separated emission spectra (33). These authors made a trade-off between the amount of cross-contamination of each acceptor considered, using various filter sets, and the transfer efficiency between Luc and the acceptors. To overcome the limitations of the filter-based strategy, we performed a full spectral decomposition of the BRET signal. Using full-spectral multiplexing, it thus became possible to assess the selective activation of TRPV1, TRPV3, and TRPV4 channels in a single sample. This opens up, to our knowledge, new prospects for evaluating the specific action of particular drugs on different TRPV subtypes within a single experiment.

Full-spectral BRET multiplexing may also be useful for monitoring several molecular events simultaneously or evaluating the kinetics of their engagement. It is known that a single receptor in the G-protein coupled receptor family engages different signaling pathways and that various drugs binding to this membrane protein may differentially influence each of them, leading to a reassessment of the efficacy concept (51). In other words, ligands that are agonists for a given signaling pathway may act as antagonists or even inverse agonists for another pathway via the same receptor. Whether this concept is also applicable to voltage-gated channels, especially TRPs, remains to be determined. The large network of protein-protein interactions in ion-channel pathways offers a rich source of potential drug targets (52). The TRPV1 channel, for example, has been shown to interact with multiple partners, such as Caveolin (53), β-Arrestin-2 (54), AKAP79/150 (55), and PKCβ2 (56), as well as other TRP channels (57). Constructing BRET probes to test the interactions between TRPV1 and each of these partners will greatly contribute to resolving the complex, dynamic interplay between TRPV1 and its interactome, thus offering, to our knowledge, new effective methods for screening

macromolecular complexes in search of new compounds that target protein-channel interfaces. In this context, monitoring multiple signaling pathways via a single multicolored assay protocol represents a highly valuable development.

This report describes an efficient technique for collecting three BRET signals simultaneously from one cell sample. Instead of using a single optical fiber to collect the photons from the sample, it is technically possible to use a bundle of many optical fibers to collect the BRET spectra from multiple samples in real time. This simultaneous recording of the dynamics of three BRET probes in many samples in parallel is likely to provide highly valuable data for drug screening. Channel-specific BRET probes for TRPV1/3/4 will lead to multi-BRET probe readings in a multiwell format, which undoubtedly represents a breakthrough in ion-channel drug screening and drug discovery in general.

SUPPORTING MATERIAL

Eight figures and one table are available at http://www.biophysj.org/biophysj/supplemental/S0006-3495(16)34266-7.

AUTHOR CONTRIBUTIONS

Y.P. and B.V. originally conceived the project; H.J.R., Y.P., and B.V. contributed to the conception and designed of the work, and wrote the article; H.J.R. and Y.P. performed the experiments and analyzed the data; G.S. coded the LabView interface for BRET spectra decomposition; F.P.d.G., E.P.-H., and A.H. helped with cell culture, transfection, and molecular biology; I.L. contributed expertise and helped finding financial support and drafting the article; P.V. helped with the calcium assays and drafting the article; and B.G., S.A., and N.S. helped with the spectral BRET signal acquisition. All authors reviewed and approved the article.

ACKNOWLEDGMENTS

We thank the Agence De l'Environnement et de la Maîtrise de l'Energie (ADEME), the Conseil Régional de l'Aquitaine, and the European Commission (FP7) (European project GERONIMO, grant agreement No. 603794) for their financial support.

REFERENCES

1. Miyawaki, A., and Y. Niino. 2015. Molecular spies for bioimaging—fluorescent protein-based probes. *Mol. Cell.* 58:632–643.
2. Ayoub, M. A. 2016. Resonance energy transfer-based approaches to study GPCRs. *Methods Cell Biol.* 132:255–292.
3. Niehörster, T., A. Löschberger, …, M. Sauer. 2016. Multi-target spectrally resolved fluorescence lifetime imaging microscopy. *Nat. Methods.* 13:257–262.
4. Grecco, H. E., S. Imtiaz, and E. Zamir. 2016. Multiplexed imaging of intracellular protein networks. *Cytometry A.* 89:761–775.
5. Clapham, D. E. 2003. TRP channels as cellular sensors. *Nature.* 426:517–524.
6. Kaneko, Y., and A. Szallasi. 2014. Transient receptor potential (TRP) channels: a clinical perspective. *Br. J. Pharmacol.* 171:2474–2507.
7. Vay, L., C. Gu, and P. A. McNaughton. 2012. The thermo-TRP ion channel family: properties and therapeutic implications. *Br. J. Pharmacol.* 165:787–801.
8. Kremers, G. J., J. Goedhart, …, T. W. Gadella, Jr. 2006. Cyan and yellow super fluorescent proteins with improved brightness, protein folding, and FRET Förster radius. *Biochemistry.* 45:6570–6580.
9. Loening, A. M., T. D. Fenn, …, S. S. Gambhir. 2006. Consensus guided mutagenesis of Renilla luciferase yields enhanced stability and light output. *Protein Eng. Des. Sel.* 19:391–400.
10. Erard, M., A. Fredj, …, F. Merola. 2013. Minimum set of mutations needed to optimize cyan fluorescent proteins for live cell imaging. *Mol. Biosyst.* 9:258–267.
11. Percherancier, Y., Y. A. Berchiche, …, N. Heveker. 2005. Bioluminescence resonance energy transfer reveals ligand-induced conformational changes in CXCR4 homo- and heterodimers. *J. Biol. Chem.* 280:9895–9903.
12. Hamdan, F. F., Y. Percherancier, …, M. Bouvier. 2006. Monitoring protein-protein interactions in living cells by bioluminescence resonance energy transfer (BRET). *Curr. Protoc. Neurosci.* Chapter 5, Unit 5.23.
13. Levenberg, K. 1944. A method for the solution of certain non-linear problems in least squares. *Quart. J. App. Math.* 2:164–168.
14. Kobrinsky, E., L. Stevens, …, N. M. Soldatov. 2006. Molecular rearrangements of the Kv2.1 potassium channel termini associated with voltage gating. *J. Biol. Chem.* 281:19233–19240.
15. Rosenbaum, T., A. Gordon-Shaag, …, S. E. Gordon. 2004. Ca^{2+}/calmodulin modulates TRPV1 activation by capsaicin. *J. Gen. Physiol.* 123:53–62.
16. Numazaki, M., T. Tominaga, …, M. Tominaga. 2003. Structural determinant of TRPV1 desensitization interacts with calmodulin. *Proc. Natl. Acad. Sci. USA.* 100:8002–8006.
17. Cheng, W., F. Yang, …, J. Zheng. 2007. Thermosensitive TRPV channel subunits coassemble into heteromeric channels with intermediate conductance and gating properties. *J. Gen. Physiol.* 129:191–207.
18. de la Rosa, V., G. E. Rangel-Yescas, …, L. D. Islas. 2013. Coarse architecture of the transient receptor potential vanilloid 1 (TRPV1) ion channel determined by fluorescence resonance energy transfer. *J. Biol. Chem.* 288:29506–29517.
19. Liao, M., E. Cao, …, Y. Cheng. 2013. Structure of the TRPV1 ion channel determined by electron cryo-microscopy. *Nature.* 504:107–112.
20. Flynn, R., K. Chapman, …, C. Altier. 2014. Targeting the transient receptor potential vanilloid type 1 (TRPV1) assembly domain attenuates inflammation-induced hypersensitivity. *J. Biol. Chem.* 289:16675–16687.
21. Mercier, J. F., A. Salahpour, …, M. Bouvier. 2002. Quantitative assessment of β1- and β2-adrenergic receptor homo- and heterodimerization by bioluminescence resonance energy transfer. *J. Biol. Chem.* 277:44925–44931.
22. Caterina, M. J., M. A. Schumacher, …, D. Julius. 1997. The capsaicin receptor: a heat-activated ion channel in the pain pathway. *Nature.* 389:816–824.
23. Cui, Y., F. Yang, …, J. Zheng. 2012. Selective disruption of high sensitivity heat activation but not capsaicin activation of TRPV1 channels by pore turret mutations. *J. Gen. Physiol.* 139:273–283.
24. McIntyre, P., L. M. McLatchie, …, I. F. James. 2001. Pharmacological differences between the human and rat vanilloid receptor 1 (VR1). *Br. J. Pharmacol.* 132:1084–1094.
25. Matta, J. A., and G. P. Ahern. 2007. Voltage is a partial activator of rat thermosensitive TRP channels. *J. Physiol.* 585:469–482.
26. Vlachová, V., A. Lyfenko, …, L. Vyklický. 2001. The effects of capsaicin and acidity on currents generated by noxious heat in cultured neonatal rat dorsal root ganglion neurones. *J. Physiol.* 533:717–728.
27. Shin, Y. C., S. Y. Shin, …, J. H. Jeon. 2012. TRIP database 2.0: a manually curated information hub for accessing TRP channel interaction network. *PLoS One.* 7:e47165.

28. Phelps, C. B., R. R. Wang, …, R. Gaudet. 2010. Differential regulation of TRPV1, TRPV3, and TRPV4 sensitivity through a conserved binding site on the ankyrin repeat domain. *J. Biol. Chem.* 285:731–740.
29. Deering-Rice, C. E., V. K. Mitchell, …, C. A. Reilly. 2014. Drofenine: a 2-APB analogue with greater selectivity for human TRPV3. *Pharmacol. Res. Perspect.* 2:e00062.
30. Jin, M., Z. Wu, …, R. G. O'Neil. 2011. Determinants of TRPV4 activity following selective activation by small molecule agonist GSK1016790A. *PLoS One*. 6:e16713.
31. Bertrand, L., S. Parent, …, L. Ménard. 2002. The BRET2/arrestin assay in stable recombinant cells: a platform to screen for compounds that interact with G protein-coupled receptors (GPCRS). *J. Recept. Signal Transduct. Res.* 22:533–541.
32. Zhang, L., F. Xu, …, W. Min. 2013. Bioluminescence assisted switching and fluorescence imaging (BASFI). *J. Phys. Chem. Lett.* 4:3897–3902.
33. Breton, B., É. Sauvageau, …, M. Bouvier. 2010. Multiplexing of multicolor bioluminescence resonance energy transfer. *Biophys. J.* 99:4037–4046.
34. Shcherbakova, D. M., M. A. Hink, …, V. V. Verkhusha. 2012. An orange fluorescent protein with a large Stokes shift for single-excitation multicolor FCCS and FRET imaging. *J. Am. Chem. Soc.* 134:7913–7923.
35. Takai, A., M. Nakano, …, T. Nagai. 2015. Expanded palette of nanolanterns for real-time multicolor luminescence imaging. *Proc. Natl. Acad. Sci. USA.* 112:4352–4356.
36. Kusch, J., and G. Zifarelli. 2014. Patch-clamp fluorometry: electrophysiology meets fluorescence. *Biophys. J.* 106:1250–1257.
37. Trudeau, M. C., and W. N. Zagotta. 2004. Dynamics of Ca^{2+}-calmodulin-dependent inhibition of rod cyclic nucleotide-gated channels measured by patch-clamp fluorometry. *J. Gen. Physiol.* 124:211–223.
38. Derler, I., M. Hofbauer, …, C. Romanin. 2006. Dynamic but not constitutive association of calmodulin with rat TRPV6 channels enables fine tuning of Ca^{2+}-dependent inactivation. *J. Physiol.* 577:31–44.
39. Biswas, S., I. Deschênes, …, G. F. Tomaselli. 2008. Calmodulin regulation of Nav1.4 current: role of binding to the carboxyl terminus. *J. Gen. Physiol.* 131:197–209.
40. Gonçalves, J. T., and W. Stühmer. 2010. Calmodulin interaction with hEAG1 visualized by FRET microscopy. *PLoS One.* 5:e10873.
41. Pfleger, K. D., and K. A. Eidne. 2006. Illuminating insights into protein-protein interactions using bioluminescence resonance energy transfer (BRET). *Nat. Methods.* 3:165–174.
42. Terstappen, G. C., R. Roncarati, …, R. Peri. 2010. Screening technologies for ion channel drug discovery. *Future Med. Chem.* 2:715–730.
43. Chambard, J. M., E. Tagat, …, M. Partiseti. 2014. Transforming TRP channel drug discovery using medium-throughput electrophysiological assays. *J. Biomol. Screen.* 19:468–477.
44. Yu, H. B., M. Li, …, X. L. Wang. 2016. High throughput screening technologies for ion channels. *Acta Pharmacol. Sin.* 37:34–43.
45. Robertson, D. N., R. Sleno, …, G. Pineyro. 2016. Design and construction of conformational biosensors to monitor ion channel activation: a prototype FlAsH/BRET-approach to Kir3 channels. *Methods.* 92:19–35.
46. Lishko, P. V., E. Procko, …, R. Gaudet. 2007. The ankyrin repeats of TRPV1 bind multiple ligands and modulate channel sensitivity. *Neuron.* 54:905–918.
47. Lau, S. Y., E. Procko, and R. Gaudet. 2012. Distinct properties of Ca^{2+}-calmodulin binding to N- and C-terminal regulatory regions of the TRPV1 channel. *J. Gen. Physiol.* 140:541–555.
48. Yang, F., Y. Cui, …, J. Zheng. 2010. Thermosensitive TRP channel pore turret is part of the temperature activation pathway. *Proc. Natl. Acad. Sci. USA.* 107:7083–7088.
49. Voets, T., K. Talavera, …, B. Nilius. 2005. Sensing with TRP channels. *Nat. Chem. Biol.* 1:85–92.
50. Nilius, B., K. Talavera, …, T. Voets. 2005. Gating of TRP channels: a voltage connection? *J. Physiol.* 567:35–44.
51. Galandrin, S., G. Oligny-Longpré, and M. Bouvier. 2007. The evasive nature of drug efficacy: implications for drug discovery. *Trends Pharmacol. Sci.* 28:423–430.
52. Stoilova-McPhie, S., S. Ali, and F. Laezza. 2013. Protein-protein interactions as new targets for ion channel drug discovery. *Austin J. Pharmacol. Ther.* 1(2), pii: 5.
53. Storti, B., C. Di Rienzo, …, F. Beltram. 2015. Unveiling TRPV1 spatiotemporal organization in live cell membranes. *PLoS One.* 10:e0116900.
54. Por, E. D., S. M. Bierbower, …, N. A. Jeske. 2012. β-Arrestin-2 desensitizes the transient receptor potential vanilloid 1 (TRPV1) channel. *J. Biol. Chem.* 287:37552–37563.
55. Zhang, X., L. Li, and P. A. McNaughton. 2008. Proinflammatory mediators modulate the heat-activated ion channel TRPV1 via the scaffolding protein AKAP79/150. *Neuron.* 59:450–461.
56. Li, L., R. Hasan, and X. Zhang. 2014. The basal thermal sensitivity of the TRPV1 ion channel is determined by PKCβII. *J. Neurosci.* 34:8246–8258.
57. Cheng, W., C. Sun, and J. Zheng. 2010. Heteromerization of TRP channel subunits: extending functional diversity. *Protein Cell.* 1:802–810.

Biophysical Journal, Volume *112*

Supplemental Information

Full-Spectral Multiplexing of Bioluminescence Resonance Energy Transfer in Three TRPV Channels

Hermanus Johannes Ruigrok, Guillaume Shahid, Bertrand Goudeau, Florence Poulletier de Gannes, Emmanuelle Poque-Haro, Annabelle Hurtier, Isabelle Lagroye, Pierre Vacher, Stéphane Arbault, Neso Sojic, Bernard Veyret, and Yann Percherancier

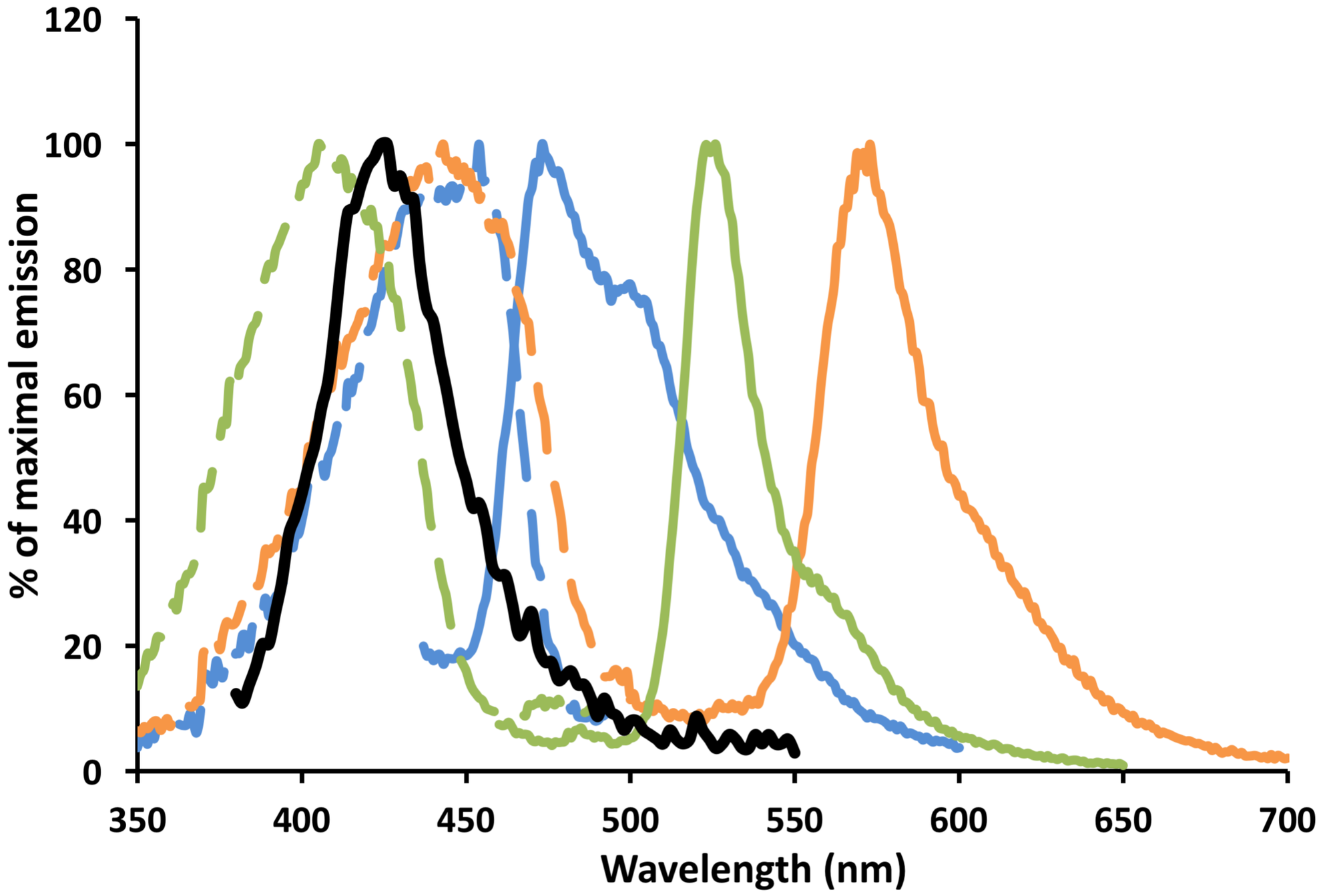

FIGURE S1 Compatibility of the emission spectrum of Luc (in the presence of purple coelenterazine substrate, black line) and the absorption (dotted lines) and emission spectra (full lines) of aquamarine (blue lines), mAmetrine (green lines), and Lss-mOrange (orange lines).

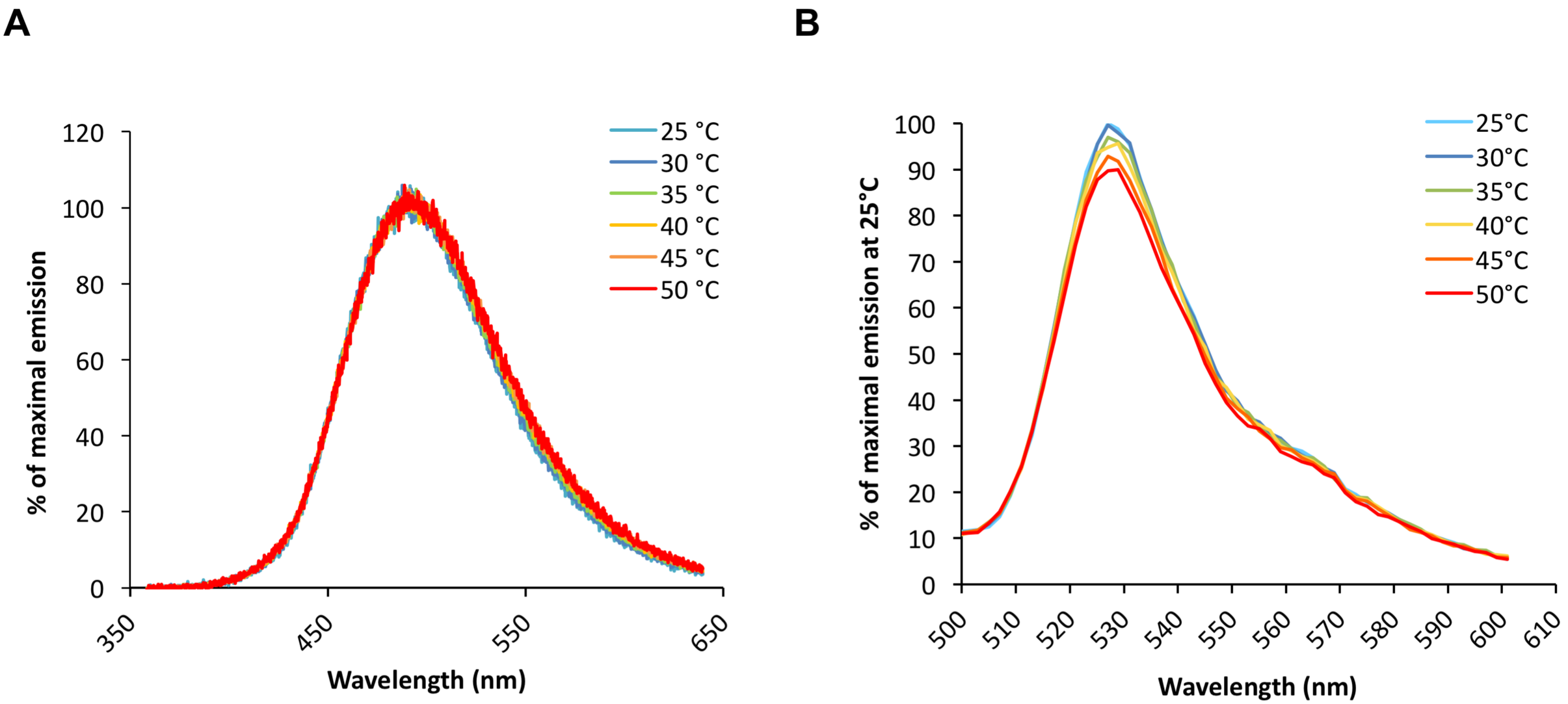

FIGURE S2 Emission spectra of Luc (in presence of Coelenterazine H) (A) and YFP (B) at temperatures ranging from 25 to 50 °C.

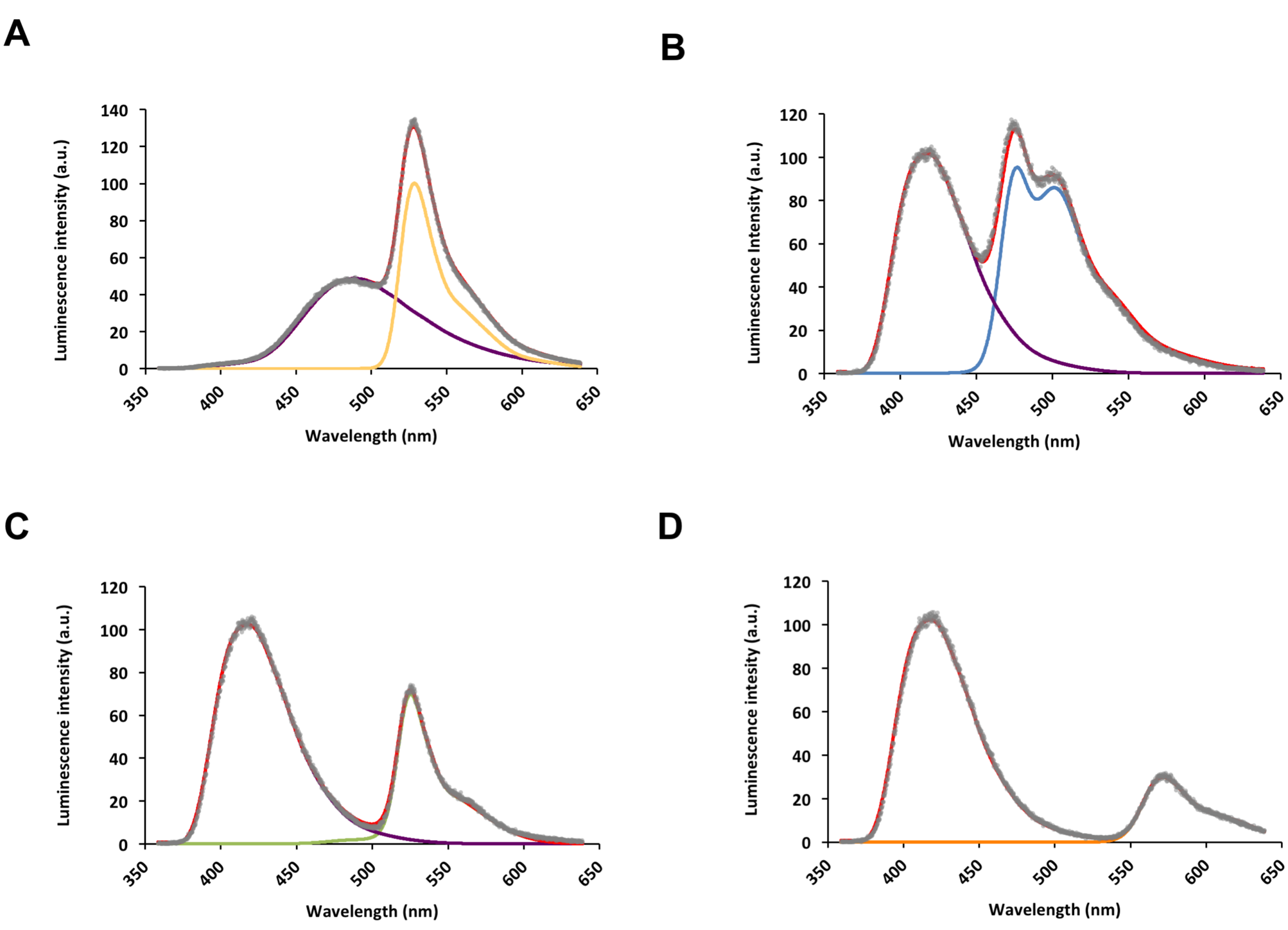

FIGURE S3 Signal decomposition of the bioluminescent spectra measured from HEK293T cells expressing YFP-Luc (A), aquamarine-Luc (B), mAmetrine-Luc (C), or LSSmOrange-Luc (D). Based on the experimental data (red line), the LabVIEW interface was used to calculate the shape of the BRET signal and separate the Luc emission spectrum (purple line) from those of YFP (yellow line, A), aquamarine (blue line, B), mAmetrine (green line, C), and LSSmOrange (orange line, D). The BRET ratio was then calculated by dividing the area under the acceptor spectrum by that under the donor spectrum, thus assuring its independence from any contamination by that of the donor or other acceptors. Net BRET for each FP-Luc is as follow: 0.82 for YFP-Luc, 1.09 for CFP-Luc, 0.43 for mAmetrine-Luc and 0.24 for LssmOrange-Luc. Coelenterazine H was used as a substrate in A, while purple coelenterazine was used as a substrate in B-D.

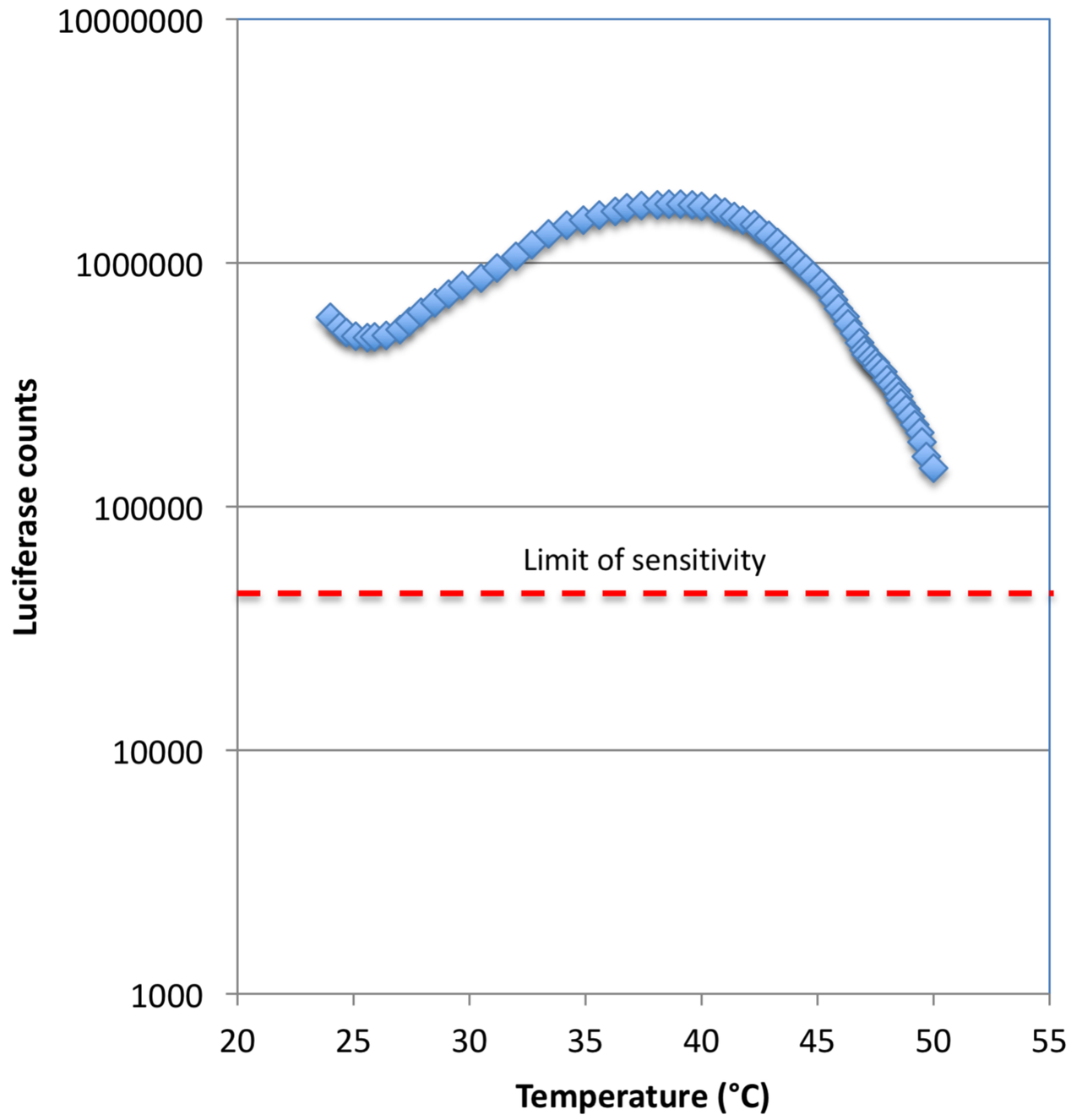

Figure S4 Effect of temperature on bioluminescence measured from live and adherent HEK293T cells expressing TRPV1-Luc. The total luciferase counts from the Luc spectra were measured after addition of 5 µM of Coelenterazine H. The measurement was performed using the Acton Spectrapro2300i. The limit of sensitivity of the spectrometer, e.g. lower number of counts below which the Luc spectra is not efficiently decomposed, is indicated as a red dashed line.

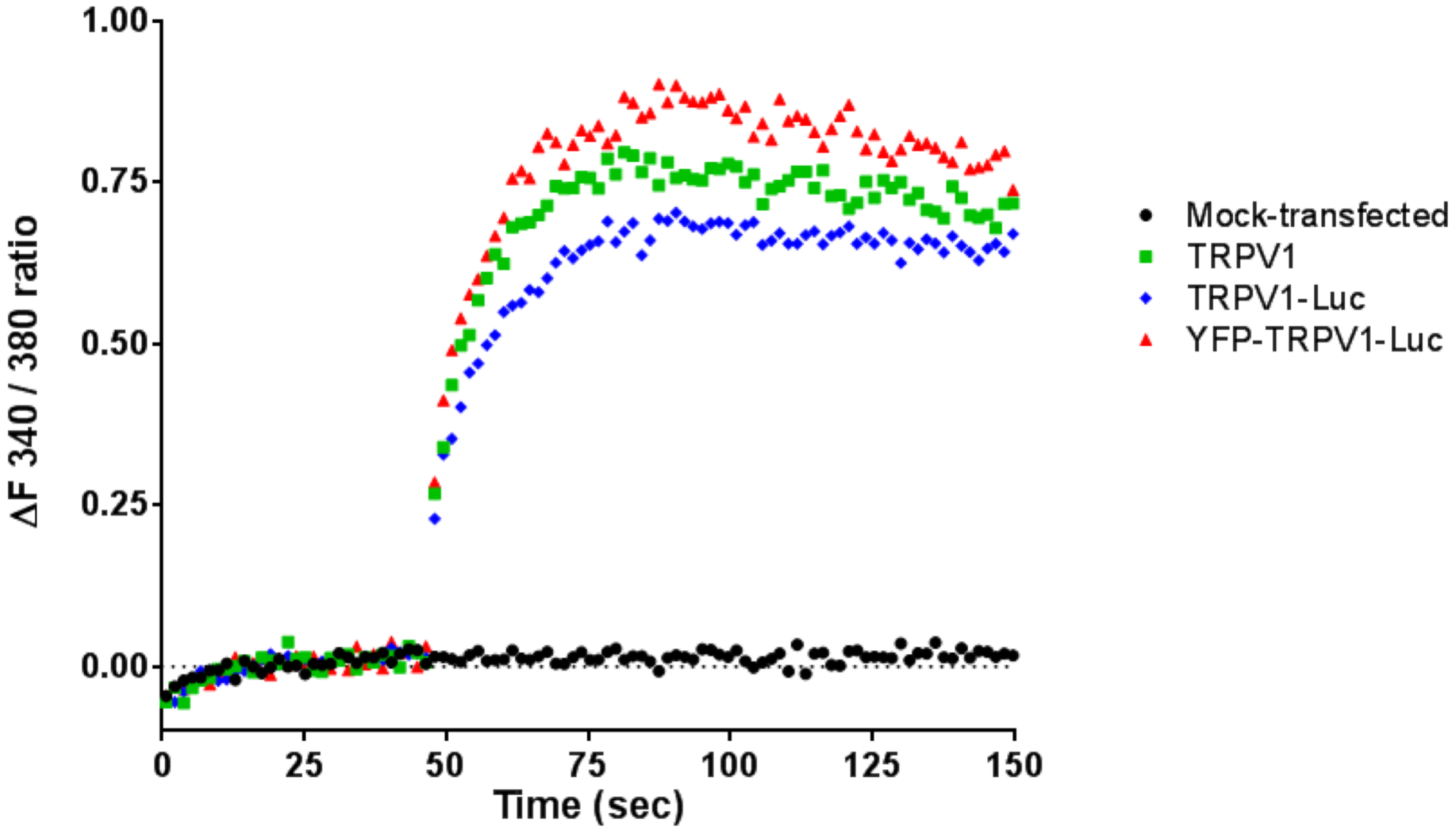

FIGURE S5 Ca^{2+} influx was induced by 20 μM capsaicin stimulation of human embryonic kidney (HEK) cells, mock-transfected or transiently expressing TRPV1, TRPV1-Luc, or YFP-TRPV1-Luc. Ca^{2+} entry was measured as a change in fluorescence intensity, before and after addition of the agonist (applied at 45 sec). The plotted signal corresponds to the difference between the 340/380 nm ratio for each dot, and the basal ratio measured in the absence of stimulation. Data represent the average of three independent experiments. Analysis yielded similar time constants under all TRPV1 transfected conditions with $\tau = 4.71 \pm 0.44$ sec for TRPV1, $\tau = 6.38 \pm 0.43$ sec for TRPV1-Luc, and $\tau = 5.02 \pm 0.51$ sec for YFP-TRPV1-Luc.

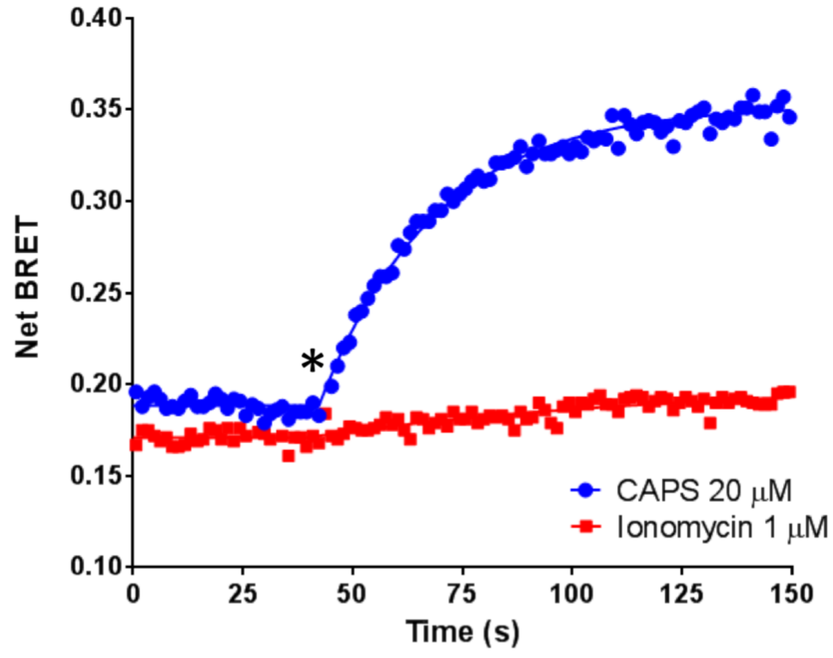

FIGURE S6 Kinetic measurement of the effect of 20 µM CAPS or 1 µM Ionomycin on cells expressing the TRPV1-Luc/YFP-CaM constructs. Compounds were injected at the time indicated by a star. Data represent one out of five independent experiments. The time-constant (τ) of the BRET increase induced by CAPS is 26.28 ± 0.95 s, n=5.

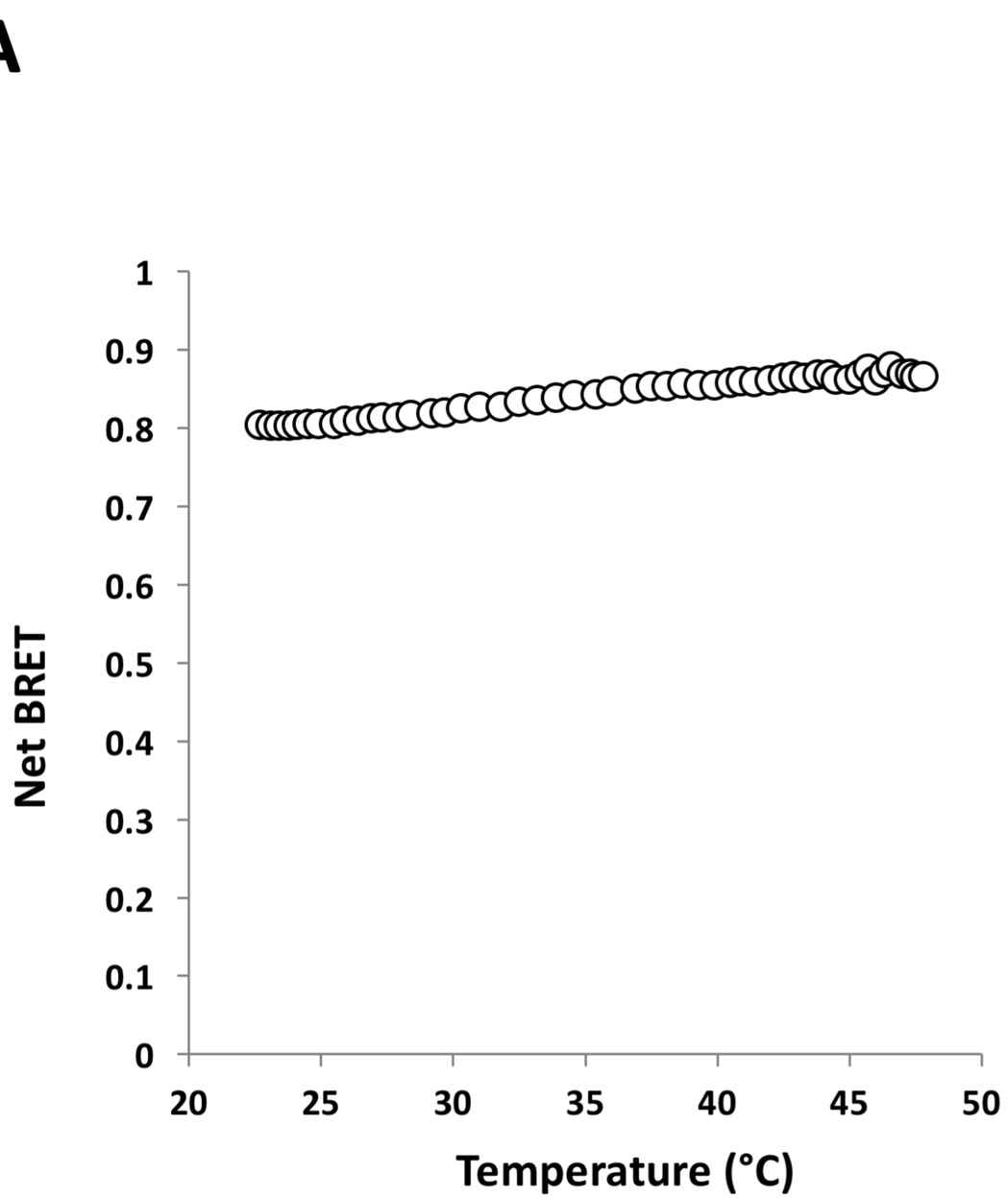

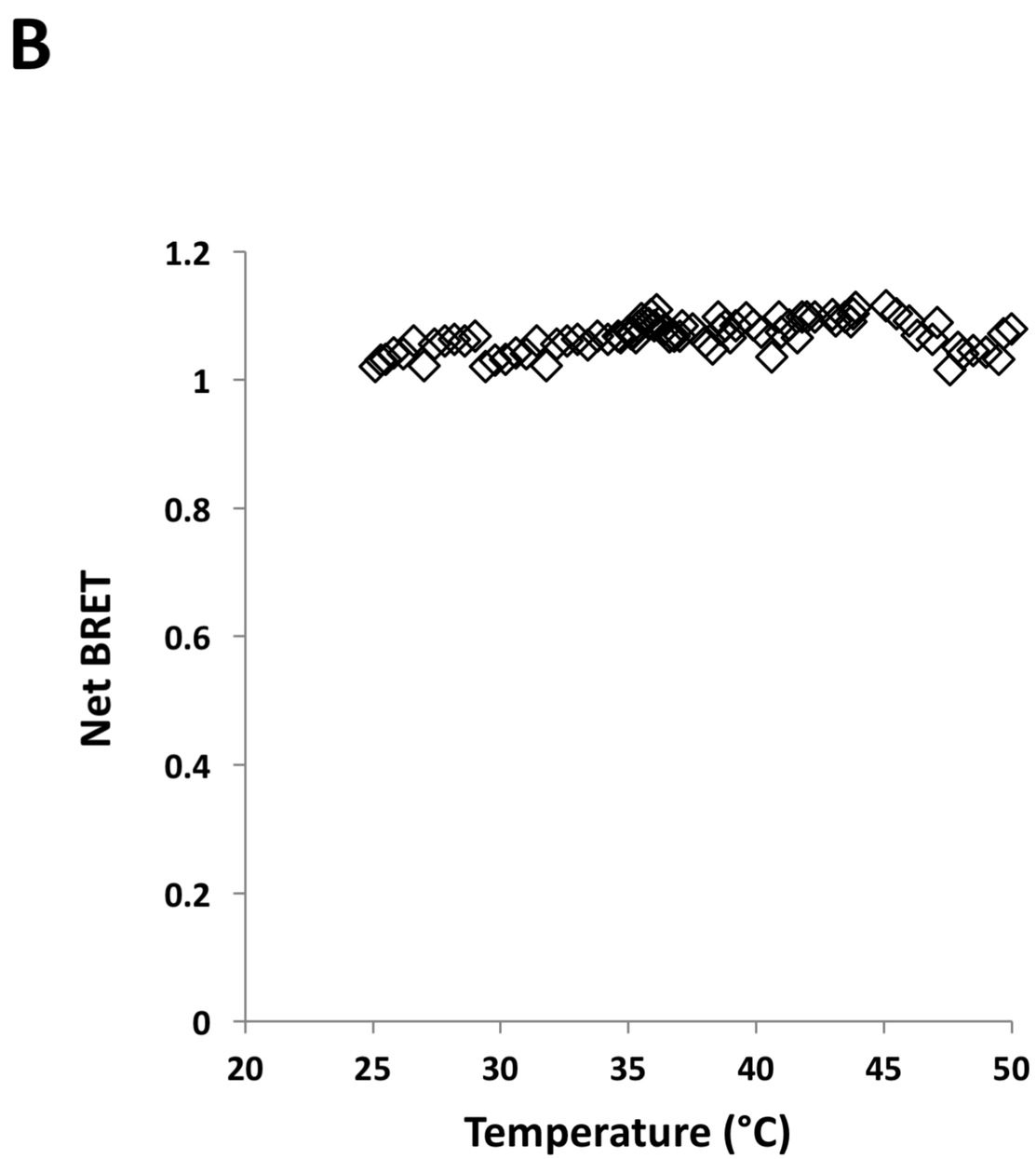

FIGURE S7 Effect of temperature on Net BRET measured on HEK293T cells transfected with YFP-Luc (A) or CD95-Luc/CD95-YFP (B).

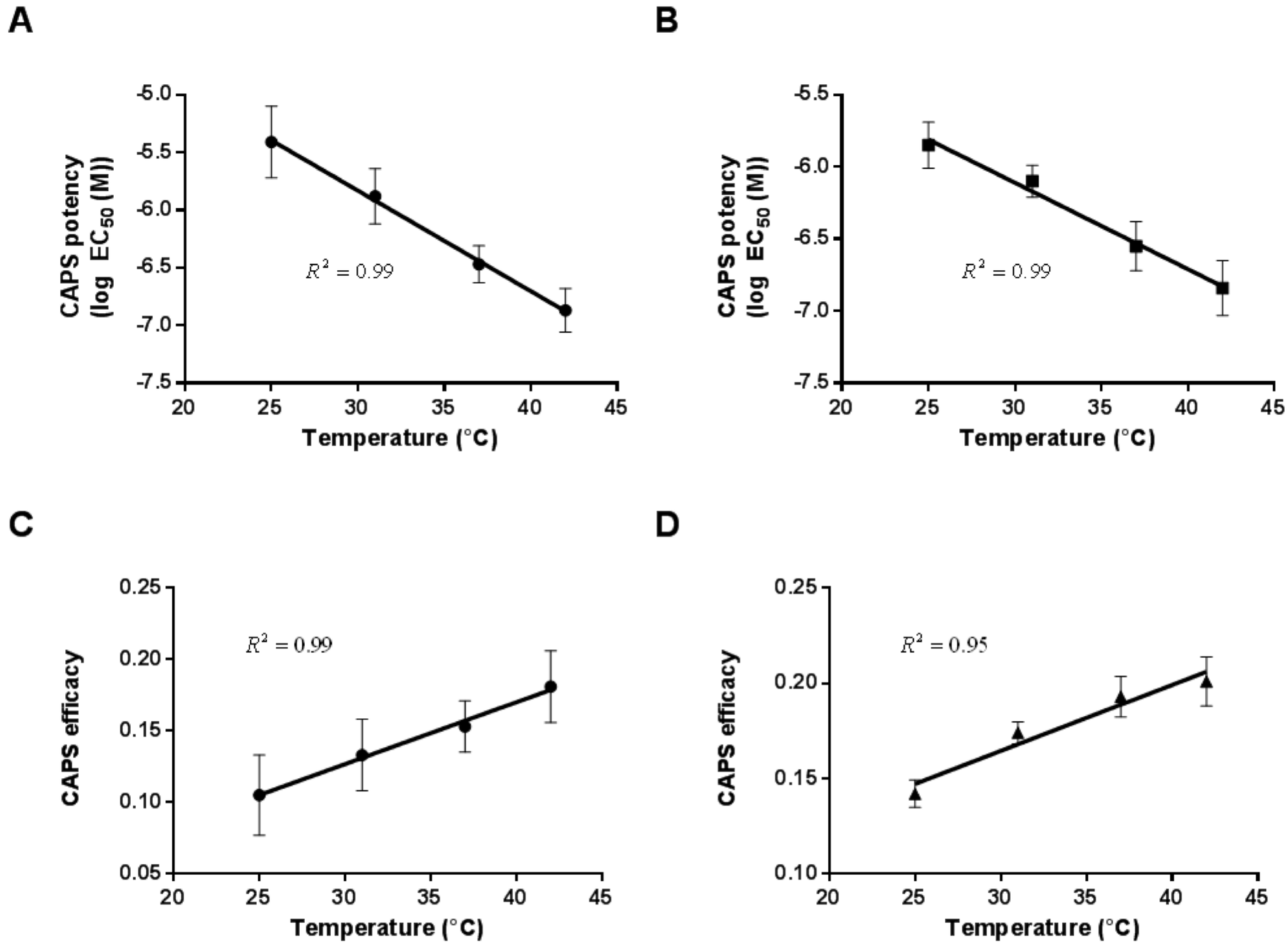

FIGURE S8 Pharmacological parameters derived from CAPS-dose response curves carried out at different temperatures in HEK293T cells expressing either YFP-TRPV1-Luc (A and C) or TRPV1-Luc/YFP-CaM BRET probes (B and D). CAPS Potency (A and B) is expressed as Log EC_{50} (M) and CAPS efficacy (B and D) is expressed as the net BRET variation between the minimum and maximum BRET values derived from sigmoidal dose-response curve fitting. Values represent the mean ± standard error of five independent experiments performed in duplicate. For each set of data, a linear regression has been performed between either CAPS potency or efficacy and the temperature. The goodness of the fit, R^2, is indicated.

Table S1 CAPS potency derived from BRET assays carried out in HEK293T expressing either YFP-TRPV1-Luc or TRPV1-Luc/YFP-CaM, activated with increasing doses of CAPS, with or without inhibitors (vehicle, CPZ 1μM, or AMG517 1 μM). BRET assays were analyzed by nonlinear regression using the GraphPad-Prism software. Potency, expressed as Log EC_{50} (M), was derived from sigmoidal dose-response curve fitting. Values represent the mean ± standard error of four independent experiments performed in duplicate. Data were analyzed against the control condition (no inhibitors) for significance using unpaired Student's t test analysis with Prism software. Asterisks indicate statistical significance of the difference between the inhibitors conditions and control condition with ****, $p < 0.0001$; ***, $p < 0.001$; **, $p < 0.01$. "ns" indicates no significant differences with the no inhibitor group ($p > 0.05$).

	Inhibitors			
	None (CAPS alone)	Vehicle	AMG517	CPZ
YFP-TRPV1-Luc	−6.50 ± 0.11	-6.44 ± 0.11^{ns}	$-5.07 \pm 0.10^{***}$	$-4.57 \pm 0.16^{**}$
TRPV1-Luc/YFP-CaM	−6.53 ± 0.16	-6.64 ± 0.14^{ns}	$-4.78 \pm 0.09^{****}$	$-4.29 \pm 0.19^{**}$